計畫編號：NHRI-GT-EX89B719L

國家衛生研究院八十九年度整合性醫藥衛生科技研究計畫

保存移植器官攜氧體之合成研究

計畫名稱

八十九年度成果報告

執 行 機 構：臺北醫學院細胞及分子生物研究所

計 畫 主 持 人：施子弼

執 行 期 間：88 年 7 月 1 日 至 89 年 6 月 30 日

計畫名稱：保存移殖器官攜氧體之合成研究

計畫編號：NHRI-GT-89B719L

執行機構：臺北醫學院細胞及分子生物研究所

計畫主持人：施子弼

研究人員：施子弼、蕭傳鐙

關鍵字：變異血紅蛋白，蛋白生理活性，基因重組工程，輸氧機能，器官保存及移植

壹、八十九年度計畫研究內容

摘要

本計畫執行主要目標是利用基因重組工程合成重組血紅蛋白能再低溫狀態具高攜氧效率，以期提高臨床醫學上器官保存應用及移植之效期。於第三年執行期間，預計完成的目標有三個部份，第一個部份是繼續完成其他變異重組血紅蛋白基因之合成與純化，第二部份是比較不同載體表達系統改進血紅蛋白之實際產量。第三個部份是氧合平衡分析系統 (Oxygen equilibrium curve) 之改進評估。

研究目的

本計畫在今年度執行期間之目標有三：(一) 以 PCR Mutagenesis 進行變異球蛋白基因之合成並純化與分析表達血紅蛋白之機能；(二) 比較不同載體表達系統改進血紅蛋白之實際產量；(三) 完成變異血紅蛋白之功能分析系統之評估與應用。至今我們完成的內容包括：(一)繼續合成不同之變異血紅蛋白基因，合成及純化經 PCR 定點突變之重組血紅蛋白；(三)利用本實驗室設計之高解析度氧結合分析系統，對於所合成之重組血紅蛋白進行蛋白特性分析，並評估系統之實際效能。本年度除了繼續合成及評估重組血

紅蛋白變異血紅蛋白株同時建立一氧合平衡系統以加強血紅蛋白輸氧機能之分析。並比較探討不同的表現系統於大量培養時血紅蛋白的產量及品質。同時，本實驗室設計了代表蛋白生理活性之氧平衡曲線檢測系統，證實對於反應數據之準確性及靈敏度上有很大的突破。

研究方法

一、氨基酸序列比較與分析

本計劃執行過程中所使用之分析軟體爲 DNASTAR Inc.之 *Lasergene* 針對 Gene Bank、Protein Data Base、Multiple Alignment 等進行一系列比對與分析的工作。找出相異的氨基酸殘基以供點突變之設計，並且利用 *Insight II*、*Biopolymer* 以及 *Discover* 等分子模擬軟體於 Silicon Graphics Indigo II 電腦下進行球蛋白之分子模擬，推定四合體之可能結構變化及影響。

二、人類血紅蛋白基因之設計及構築

由 mRNA 經 RT-PCR 合成人類血紅蛋白 cDNA ，參考人類血紅蛋白序列及大腸桿菌之氨基酸轉譯密碼使用頻率合成重組血紅蛋白基因。

三、進行點突變之聚合酶鏈鎖反應與表達蛋白載體之構築

首先將血紅蛋白於軟體 *DNASTAR* 中分析限制鏈鎖反應之點突變進行與表達載體之構築限制酶切位，在將設計點突變的位置附近，查看是否切位有所改變或增減。最後設計適當之引子，以原始人類血紅蛋白基因爲模板，*GeneAmp PCR System 2400* 中進行合成反應，將合成

之 PCR 產物經適當限制酶切割後轉載入質體如 pKK233-2 中，經由 DNA 定序工作確認變異序列無誤後，進行變異血紅蛋白之菌體內大量表達的工作。

四、血紅蛋白之分離與純化

本計劃之蛋白分離過程依序使用 FPLC 膠質層析(Gel filtration)、陽離子交換樹脂 CM-52、陰離子交換樹脂 DEAE 及 Resource-S 陽離子親和交換分離管柱純化合成蛋白。分離過程中應用光譜波長的吸收區域變化來確認純化的程度，最後利用 Cellulose Acetate 進行血紅蛋白電泳分析，確認氨基酸改變後對於分子帶電性的影響及蛋白的純度。

五、血紅蛋白四合體之特性分析與功能測定

(I) 四合體之 Stability

以不同濃度之血紅蛋白進行膠質層析，並比較不同變異血紅蛋白血基質（heme）之穩定性。

(II) 攜氧機能分析

經過陰離子交換樹脂純化及電泳確認後，將濃縮的血紅蛋白進行氧合平衡曲線分析（Oxygen Equilibrium Curve）。定義氧分子與血紅蛋白四合體結合的飽合度 Y 爲縱軸，氧氣分壓 Po_2 爲衡軸，測定後得到一氧合解離曲線圖（Oxygen Dissociation Curve）。以其 50%氧飽和之氧分壓（P_{50}）爲其攜氧參數並由解離平衡式 $Hb(O_2)n \rightarrow Hb+nO_2$，就其協同性質（Coopericity）造成的 S 曲線，取對數值後作 log[T/1-Y]對 $logPo_2$ 作圖，得到 Hill 係數值 n 分別以不同的變異血紅蛋白進行測試。

(III) 血紅蛋白氧合平衡曲線測定

利用陰陽離子樹脂分離純化的血紅蛋白在經過濃縮後，利用聚光燈照射同時通入氧氣作低溫氣體交換，使血紅蛋白與氧氣結合，置換於不同的緩衝溶液中，測定氧合曲線。

(i) Temperature effect

計算各溫度之ΔH=2.303 x R x Δlog50/Δ(1/T)數值（T 代表不同溫度），相較於正常蛋白決定變異蛋白之溫度敏感性。

(ii) Bohr effect

在不同的 pH 值變化時，計錄因溫度改變的不同 P_{50} 而計算出對應之 $\Delta log_{50}/\Delta pH$ 值。

(iii) Anion effect

針對輔助因子（Allosteric cofactor）如 Cl^-，PO_4^{3-} 等對血紅蛋白攜氧機能之影響作分析，以 $\Delta logP_{50}/\Delta log[anion]$ 值定量之。

(vi) Oxydation rate

取適量之血紅蛋白利用分光分度計，在特定波長下加入氧化劑以偵測氧化速率，再繪出完整氧化曲線。

研究結果

（一） 重組變異株之基因合成純化蛋白之分析

在單變異血紅蛋白部份於 external 區域增加了β6(NA6)E→K; 在雙重變異部份增加了β2(NA2)H→β6(NA6)E→K 及三重變異部份β2(NA2)H→E+β6(NA6)E→K+β82(EF6)K→N，四重變異部份爲β2(NA2)H→E+β6(NA6)E→K+β82(EF6)K→N+β108(G10)N→D 變異

株之基因構築及蛋白合成，增進對於特定胺基酸與不同胺基酸之加成效應有更具體的瞭解。氧合平衡實驗結果顯示包含於中央空腔及蛋白表面之雙重變異株 β2(NA2)H→E+β6(NA6)E→K 其輸氧機能明顯的對溫度變化敏感度減低，表示溫度變化對於變異蛋白之生理活性影響較小。同時此變異株之輸氧機能較野生株高。此雙重變異株之四合體的穩定性低於人類血紅蛋白，但高於野生株之人類重組血紅蛋白。

（二）血紅蛋白於菌體內表達量之比較

爲了增進血紅蛋白之菌體表達量，已將血紅蛋白基因分別構築於 JM105/pKK223-3 (pDLIII13e) 、 JM105/pKK233-2 (BH) 、 BL21/pET29 (B5)及 M15/pQE60 (60Hb)四個不同的表達系統上（圖一 ~ 四）。變異株蛋白利用不同的系統分別進行大量（4L）菌體培養，合成蛋白經蛋白分離及純化後，所得到的血紅蛋白產量較預期相近或較低。產物的穩定性在除了原始表現系統 (pKK233-2, pKK223-3) 外，皆有降低的現象。甚或降至 60% (pET)。

（三）氧合平衡分析系統(OEC)之改進評估

本計畫於年度執行期間，爲提昇測定氧合分析系統之效率及準確性，在硬體方面，設計並製作了 OEC 氧氣平衡分析瓶，縮小體積以減少蛋白反應物之使用量。並設計了具控溫及 magnetic stir 雙重功能之樣品載台。在軟體方面，修改了資料分析程式使可 IBM PC 在中執行，以分析實驗數據資料。此系統爲國際目前唯一之系統，將經過純化之血紅蛋白實際測試後，發現其靈敏度及準確性皆很高。改進分析系統之成效目前正評估中 （見附錄）。

研究結果討論

（一）本年度合成二重及多重變異血紅蛋白，以期觀察重組蛋白對於不同環境溫度變化及安定性之加成及消減關連性。並針對未來一年計畫進行重組血紅蛋白之動物體內活性檢測提供了較具代表性的材料。

（二）對於血紅蛋白基因表達系統之重建，依結果顯示有顯著增加重組蛋白合成量，但與舊系統表達之蛋白活性及安定性比較目前正在評估中。目前純化流程已能得到非常高純度之蛋白，因此對於蛋白之活性及機能分析，可增加其準確性與可性度。

（表一）

註：粗體標示為本計畫今年度研究成果

血紅蛋白	變異株基因合成	核酸序列確定	蛋白合成及純化	機能分析 (P_{50},n_{50},$\triangle H^+$)	特性分析	其他
A)工程重組蛋白						
(I)Single-mutation						
(i)Heme Pocket						
β67(E11)V→I	Completed	Completed	Completed	~n O_2		
(ii)Subunit Interphase						
α38(C3)T→Q	Completed	Completed	Completed	↑ O_2, ↓ n	↑ tetrameric stability	
α86(F7)L→T	**Completed**	**Completed**	**>90% pure**	**~n O_2**		
α91(FG3)L→H	Completed	Completed	Completed	↓ O_2		
β91(F7)L→T	Completed	Completed	Completed	↓ O_2		
β96(FG3)L→H	**Completed**	**Completed**	**Completed**	**~n O_2**		
(iii)A Helix Region						
β11(A8)V→F	Completed	Completed	>70%	↓ O_2		
(iv)Central Cavity Region						
β2(NA2)H→E	Completed	Completed	Completed	↓ *ΔH*, ↑ O_2,,	↓ *tetrameric stability*	
β82(EF6)K→N	Completed	Completed	Completed	↑ O_2, ↓ n ↓ *ΔH*	↑ tetrameric stability	
β108(G10)N→D	Completed	Completed	Completed	In Progress		
α99(G6) K→I	**Completed**	**Completed**	**Completed**			
α94(G1) D→I	**Completed**	**Completed**				
α94(G1) D→Y	**Completed**	**Completed**	**Completed**	**In progress**		
α76(E20) M→L	Completed	Completed	Completed	↓ O_2, ↓ n		
β101(G3) E→D	Completed					
β143(H21) H→R	Completed					
(v)External						
β73(E17) D→R	Completed	**Completed**				
β83(EF7) G→E	Completed	**Completed**				
(II)Double-mutation						
α38(C3) T→Q β67(E11) V→I	Completed	Completed	**Completed**	**In progress**		
α76(E20) M→L β82(EF6) K→N	Completed	Completed	**Completed**	**In progress**		

血紅蛋白	變異株基因合成	核酸序列確定	蛋白合成及純化	機能分析 (P_{50},n_{50},$\triangle H^+$)	特性分析	其他
{α76(E20) M→L β108(G10) N→D	Completed	Completed	Completed	**In progress**		
{**β2(NA2) H→E** **β6(NA6) E→K**	**Completed**	**Completed**	**Completed**	***↓ΔH, ↑O_2,,***	***↓ tetrameric stability***	
(III)Triple-mutation						
{**α76(E20) M→L** **β2(NA2) H→E** **β108(G10) N→D**	**Completed**	**Completed**	**Completed**	**In progress**		
{**α76(E20) M→L** **β2(NA2) H→E** **β82(EF6) K→N**	**Completed**	**Completed**	**Completed**	**In progress**		
{**β108(G10) N→D** **β2(NA2) H→E** **β6(NA6) E→K**	**Completed**	**Completed**	**Completed**	**In progress**		
{**β108(G10) N→D** **β2(NA2) H→E** **β82(EF6) K→N**	**Completed**	**Completed**	**Completed**	**↓ O_2,**		
B)天然蛋白						
Channa maculata Hb	Completed	Completed	>90%	Completed ↓ O_2, ↓ $\triangle H^+$	Stable Tetramer	no root effect
Hb Old Dominion		Completed	Completed	Completed		
Hb Chico β66 Lys→Thr		Completed	Completed	Completed		JBC (1998)
C)化學合成蛋白						
Double Cross Linked Hb	化學合成	N/A	>90%	Completed		學會發表, JBC(1996) 271,(2)675-680

貳、八十九年計畫著作一覽表

群體計畫(PPG)者，不論是否提出各子計畫資料，都必須提出總計畫整合之資料
若爲群體計畫，請勾選本表屬於：☐子計畫　　☐總計畫(請自行整合)

列出貴計畫於全程計畫中之所有計畫產出於下表，包含已發表或已被接受發表之文獻、已取得或被接受之專利、擬投稿之手稿（manuscript）以及專著等。「計畫產出名稱」欄位請依「臺灣醫誌」參考文獻方式撰寫；「產出型式」欄位則填寫該產出爲期刊、專利、手稿或專著等，舉例如下：

序號	計畫產出名稱	產出型式	SCI*	致謝與否
例	Chang SF, Cheng CL. The suppression effect of DNA sequences within the C4A region on the transcription activity of human cyp21. Endocrine Research. 1998, 24(3&4):625-630	期刊	✓	✓
1.	Celia Bonaventura, and Joseph Bonaventura, **Daniel Tzu-bi Shih**, E. Timothy Iben, Joel Friedman. (1999) Altered Ligand Rebinding Kinetics Due to Distal Side Effects in Hemoglobins Chico (Lys E10 66β→Thr). *J. Biol. Chem.* **274**: 8686-8693. (SCI)	期刊	✓	
2.	Shing-Jing Chen, Yu-Hsing Chang, Jui-Shin Lin and **Daniel Tzu-Bi Shih**. High Efficient PCR Mutagenesis and Prokaryotic Expression of Recombinant Hb c-DNA. 8th symposium on Recent Advances in Cellular and Molecular Biology. Jan 29-31, 2000	研討會論文		
3.	Yu-Hsing Chang and **Daniel Tzu-Bi Shih**. Application of A High Resolution FPLC to the Analysis and Purification of Cellular Hemoglobin Derivatives and Variants. The 13th Joint Annual Conference of Biomedical Sciences, April 10-11, 1999.	研討會論文		
4.	Shing-Jing Chen, Yu-Hsing Chang, Chin-Long Huang and **Daniel Tzu-Bi Shih**. A Study on the Synthesis of Genetic Engineered Recombinant Hemoglobin with Better Quality in *E. Coli*. 7th symposium on Recent Advances in Cellular and Molecular Biology. Jan 31-Feb. 1, 1999.	研討會論文		
5.				
6.				
7.				
8.				

*SCI：Science Citation Index，若發表之期刊爲 SCI 所包含者，請打勾。

*「致謝與否」欄位：若該成果產出有註明衛生署或國家衛生研究院委託資助字樣者，請打勾。

*本表如不敷使用，請自行影印。

參、八十九年計畫所培訓之研究人員

群體計畫(PPG)者，不論是否提出各子計畫資料，都必須提出總計畫整合之資料
若爲群體計畫，請勾選本表屬於：□子計畫　　□總計畫(請自行整合)

種類			人數	備註
專任人員	1. 博士後研究人員	訓練中		
		已結訓		
	2. 碩士級研究人員	訓練中		
		已結訓	1	
	3. 學士級研究人員	訓練中		
		已結訓	2	
	4. 其他	訓練中		
		已結訓	1	
兼任人員	1. 博士班研究生	訓練中	1	
		已結訓		
	2. 碩士班研究生	訓練中	2	
		已結訓		
醫師		訓練中		
		已結訓		
特殊訓練課程				

註：1.特殊訓練課程請於備註欄說明所訓練課程名稱

2.本表如不敷使用，請自行影印

肆、八十九年計畫重要研究成果產出統計表

群體計畫(PPG)者，不論是否提出各子計畫資料，都必須提出總計畫整合之資料
若爲群體計畫，請勾選本表屬於: □子計畫　　□總計畫(請自行整合)

(係指執行全程計畫之所有研究產出成果)

科技論文篇數			技術移轉			技術報告
	國內	國外	類型	經費	項數	篇
期刊論文	篇	1篇	技術輸入	千元	項	技術創新 項
研討會論文	3篇	篇	技術輸出	千元	項	著作權(核准) 項
專著	篇	篇	技術擴散	千元	項	專利權(核准) 項

〔註〕:

期刊論文：指在學術性期刊上刊登之文章，其本文部份一般包含引言、方法、結果、及討論，並且一定有參考文獻部分，未在學術性期刊上刊登之文章（研究報告等）與博士或碩士論文，則不包括在內。

研討會論文：指參加學術性會議所發表之論文，且尚未在學術性期刊上發表者。

專　　著：爲對某項學術進行專門性探討之純學術性作品。

技術報告：指從事某項技術之創新、設計及製程等研究發展活動所獲致的技術性報告且未公開發表者。

技術移轉：指技術由某個單位被另一個單位所擁有的過程。我國目前之技術轉移包括下列三項：一、技術輸入。二、技術輸出。三、技術擴散。

技術輸入：藉僑外投資、與外國技術合作、投資國外高科技事業等方式取得先進之技術引進國內者。

技術輸出：指直接供應國外買主具生產能力之應用技術、設計、顧問服務及專利等。我國技術輸出方包括整廠輸出、對外投資、對外技術合作及顧問服務等四種。

技術擴散：指政府引導式的技術移轉方式，即由財團法人、國營事業或政府研究機構將其開發之技術擴散至民間企業之一種單向移轉（政府移轉民間）。

技術創新：指研究執行中產生的技術，且有詳實技術資料文件者。

伍、參與本計畫所有人力之職級分析

群體計畫(PPG)者，不論是否提出各子計畫資料，都必須提出總計畫整合之資料
若爲群體計畫，請勾選本表屬於: □子計畫　　□總計畫(請自行整合)

職級	所含職級類別	參與人次
第一級	研究員、教授、主治醫師	1人
第二級	副研究員、副教授、總醫師	1人
第三級	助理研究員、講師、住院醫師	人
第四級	研究助理、助教、實習醫師	3人
第五級	技術人員	人
第六級	支援人員	人
合計		5人

〔註〕

第一級：研究員、教授、主治醫師、簡任技正，若非以上職稱則相當於博士滿三年、碩士滿六年、或學士滿九年之研究經驗者。

第二級：副研究員、副教授、助研究員、助教授、總醫師、薦任技正，若非以上職稱則相當於博士、碩士滿三年、學士滿六年以上之研究經驗者。

第三級：助理研究員、講師、住院醫師、技士，若非以上職稱則相當於碩士、或學士滿三年以上之研究經驗者。

第四級：研究助理、助教、實習醫師，若非以上職稱則相當於學士、或專科滿三年以上之研究經驗者。

第五級：指目前在研究人員之監督下從事與研究發展有關之技術性工作，且具備下列資格之一者屬之：具初（國）中、高中（職）、大專以上畢業者，或專科畢業目前從事研究發展，經驗未滿三年者。

第六級：指在研究發展執行部門參與研究發展有關之事務性及雜項工作者，如人事，會計、秘書、事務人員及維修、機電人員等。

陸、參與本計畫所有人力之學歷分析

群體計畫(PPG)者，不論是否提出各子計畫資料，都必須提出總計畫整合之資料
若爲群體計畫，請勾選本表屬於: □子計畫　　□總計畫(請自行整合)

類別	學歷別	參與人次
1	博士	2人
2	碩士	1人
3	學士	1人
4	專科	1人
5	博士班研究生	人
6	碩士班研究生	2人
7	其他	人
合計		7人

柒、參與本計畫之所有協同合作之研究室

群體計畫(PPG)者，不論是否提出各子計畫資料，都必須提出總計畫整合之資料
若爲群體計畫，請勾選本表屬於: □子計畫　　□總計畫(請自行整合)

機構	研究室名稱	研究室負責人
中研院分生所	巨分子化學實驗室	蕭傳鐙

捌、八十九年計畫之完整著作抽印本或手稿

依「參、八十九年計畫著作一覽表」所列順序附上文獻抽印本或手稿。

8987196

參、八十九年計畫著作一覽表

群體計畫(PPG)者，不論是否提出各子計畫資料，都必須提出總計畫整合之資料
若爲群體計畫，請勾選本表屬於：□子計畫　　□總計畫(請自行整合)

列出貴計畫於全程計畫中之所有計畫產出於下表，包含已發表或已被接受發表之文獻、已取得或被接受之專利、擬投稿之手稿（manuscript）以及專著等。「計畫產出名稱」欄位請依「臺灣醫誌」參考文獻方式撰寫；「產出型式」欄位則填寫該產出爲期刊、專利、手稿或專著等，舉例如下：

序號	計畫產出名稱	產出型式	SCI*	致謝與否
例	Chang SF, Cheng CL. The suppression effect of DNA sequences within the C4A region on the transcription activity of human cyp21. Endocrine Research. 1998, 24(3&4):625-630	期刊	✓	✓
1.	Celia Bonaventura, and Joseph Bonaventura, **Daniel Tzu-bi Shih**, E. Timothy Iben, Joel Friedman. (1999) Altered Ligand Rebinding Kinetics Due to Distal Side Effects in Hemoglobins Chico (Lys E10 66β→Thr). *J. Biol. Chem.* 274: 8686-8693. (SCI)	期刊	✓	
2.	Shing-Jing Chen, Yu-Hsing Chang, Jui-Shin Lin and **Daniel Tzu-Bi Shih**. High Efficient PCR Mutagenesis and Prokaryotic Expression of Recombinant Hb c-DNA. 8th *symposium on* Recent Advances in Cellular and Molecular Biology. Jan 29-31, 2000	研討會論文		
3.	Yu-Hsing Chang and **Daniel Tzu-Bi Shih**. Application of A High Resolution FPLC to the Analysis and Purification of Cellular Hemoglobin Derivatives and Variants. The 13th Joint Annual Conference of Biomedical Sciences, April 10-11, 1999.	研討會論文		
4.	Shing-Jing Chen, Yu-Hsing Chang, Chin-Long Huang and **Daniel Tzu-Bi Shih**. A Study on the Synthesis of Genetic Engineered Recombinant Hemoglobin with Better Quality in *E. Coli*. 7th symposium on Recent Advances in Cellular and Molecular Biology. Jan 31-Feb. 1, 1999.	研討會論文		
5.				
6.				
7.				
8.				

*SCI：Science Citation Index，若發表之期刊爲 SCI 所包含者，請打勾。

*「致謝與否」欄位：若該成果產出有註明衛生署或國家衛生研究院委託資助字樣者，請打勾。

*本表如不敷使用，請自行影印。

肆、八十九年計畫所培訓之研究人員

群體計畫(PPG)者，不論是否提出各子計畫資料，都必須提出總計畫整合之資料
若爲群體計畫，請勾選本表屬於：☐子計畫　　☐總計畫(請自行整合)

種類			人數	備註
專任人員	1. 博士後研究人員	訓練中		
		已結訓		
	2. 碩士級研究人員	訓練中		
		已結訓	1	
	3. 學士級研究人員	訓練中		
		已結訓	2	
	4. 其他	訓練中		
		已結訓	1	
兼任人員	1. 博士班研究生	訓練中	1	
		已結訓		
	2. 碩士班研究生	訓練中	2	
		已結訓		
醫師		訓練中		
		已結訓		
特殊訓練課程				

註：1.特殊訓練課程請於備註欄說明所訓練課程名稱

2.本表如不敷使用，請自行影印

伍、八十九年計畫重要研究成果產出統計表

群體計畫(PPG)者，不論是否提出各子計畫資料，都必須提出總計畫整合之資料

若爲群體計畫，請勾選本表屬於: □子計畫　　□總計畫(請自行整合)

(係指執行全程計畫之所有研究產出成果)

科技論文篇數			技術移轉			技術報告
	國內	國外	類型	經費	項數	篇
						技術創新
期刊論文	篇	1篇	技術輸入	千元	項	項
						著作權
研討會論文	3篇	篇	技術輸出	千元	項	(核准) 項
						專利權
專著	篇	篇	技術擴散	千元	項	(核准) 項

〔註〕:

期刊論文：指在學術性期刊上刊登之文章，其本文部份一般包含引言、方法、結果、及討論，並且一定有參考文獻部分，未在學術性期刊上刊登之文章（研究報告等）與博士或碩士論文，則不包括在內。

研討會論文：指參加學術性會議所發表之論文，且尚未在學術性期刊上發表者。

專　　著：爲對某項學術進行專門性探討之純學術性作品。

技術報告：指從事某項技術之創新、設計及製程等研究發展活動所獲致的技術性報告且未公開發表者。

技術移轉：指技術由某個單位被另一個單位所擁有的過程。我國目前之技術轉移包括下列三項：一、技術輸入。二、技術輸出。三、技術擴散。

技術輸入：藉僑外投資、與外國技術合作、投資國外高科技事業等方式取得先進之技術引進國內者。

技術輸出：指直接供應國外買主具生產能力之應用技術、設計、顧問服務及專利等。我國技術輸出方包括整廠輸出、對外投資、對外技術合作及顧問服務等四種。

技術擴散：指政府引導式的技術移轉方式，即由財團法人、國營事業或政府研究機構將其開發之技術擴散至民間企業之一種單向移轉（政府移轉民間）。

技術創新：指研究執行中產生的技術，且有詳實技術資料文件者。

陸、參與本計畫所有人力之職級分析

群體計畫(PPG)者，不論是否提出各子計畫資料，都必須提出總計畫整合之資料
若爲群體計畫，請勾選本表屬於: □子計畫　　□總計畫(請自行整合)

職級	所含職級類別	參與人次
第一級	研究員、教授、主治醫師	1人
第二級	副研究員、副教授、總醫師	1人
第三級	助理研究員、講師、住院醫師	人
第四級	研究助理、助教、實習醫師	3人
第五級	技術人員	人
第六級	支援人員	人
合計		5人

〔註〕

第一級：研究員、教授、主治醫師、簡任技正，若非以上職稱則相當於博士滿三年、碩士滿六年、或學士滿九年之研究經驗者。

第二級：副研究員、副教授、助研究員、助教授、總醫師、薦任技正，若非以上職稱則相當於博士、碩士滿三年、學士滿六年以上之研究經驗者。

第三級：助理研究員、講師、住院醫師、技士，若非以上職稱則相當於碩士、或學士滿三年以上之研究經驗者。

第四級：研究助理、助教、實習醫師，若非以上職稱則相當於學士、或專科滿三年以上之研究經驗者。

第五級：指目前在研究人員之監督下從事與研究發展有關之技術性工作，且具備下列資格之一者屬之：具初（國）中、高中（職）、大專以上畢業者，或專科畢業目前從事研究發展，經驗未滿三年者。

第六級：指在研究發展執行部門參與研究發展有關之事務性及雜項工作者，如人事，會計、秘書、事務人員及維修、機電人員等。

柒、參與本計畫所有人力之學歷分析

群體計畫(PPG)者，不論是否提出各子計畫資料，都必須提出總計畫整合之資料
若爲群體計畫，請勾選本表屬於: □子計畫　　□總計畫(請自行整合)

類別	學歷別	參與人次
1	博士	2人
2	碩士	1人
3	學士	1人
4	專科	1人
5	博士班研究生	人
6	碩士班研究生	2人
7	其他	人
合計		7人

捌、參與本計畫之所有協同合作之研究室

群體計畫(PPG)者，不論是否提出各子計畫資料，都必須提出總計畫整合之資料
若爲群體計畫，請勾選本表屬於: □子計畫　　□總計畫(請自行整合)

機構	研究室名稱	研究室負責人
中研院分生所	巨分子化學實驗室	蕭傳鐙

玖、八十九年計畫之完整著作抽印本或手稿

依「參、八十九年計畫著作一覽表」所列順序附上文獻抽印本或手稿。

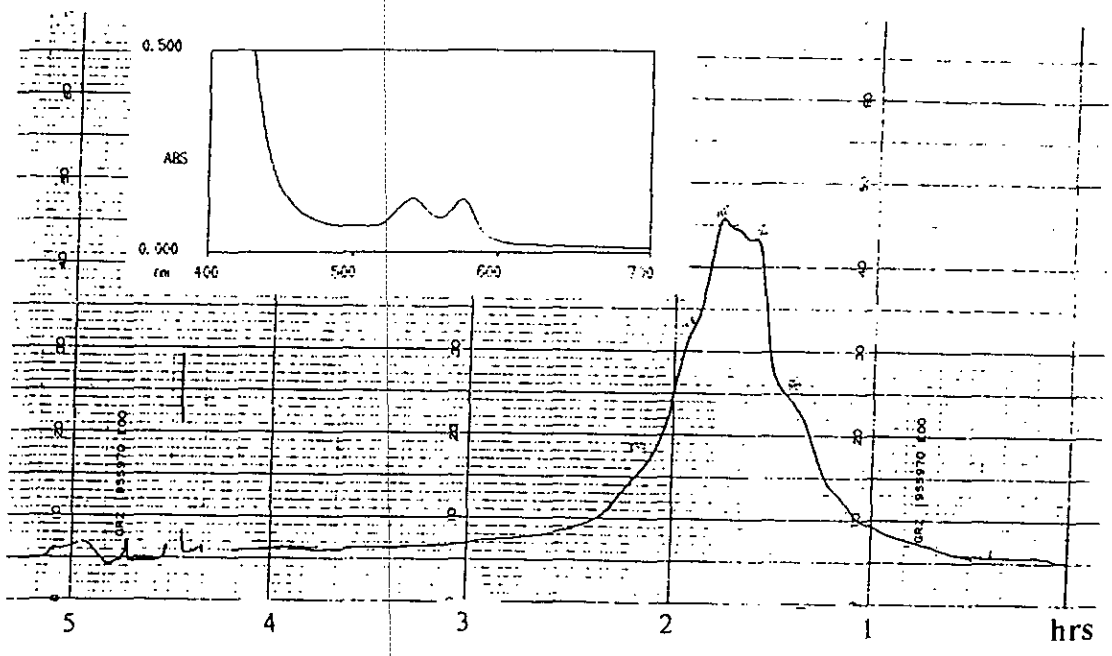

圖一 Control Hb A pKK223-2 細胞抽出物經 Resourse S 陽離子交換層析所得之分離曲線圖。左上方插圖是經 Resourse S 管柱溶離出來的 Peak 之 Visible spectrum, 從波長 400→700 nm 之結果。

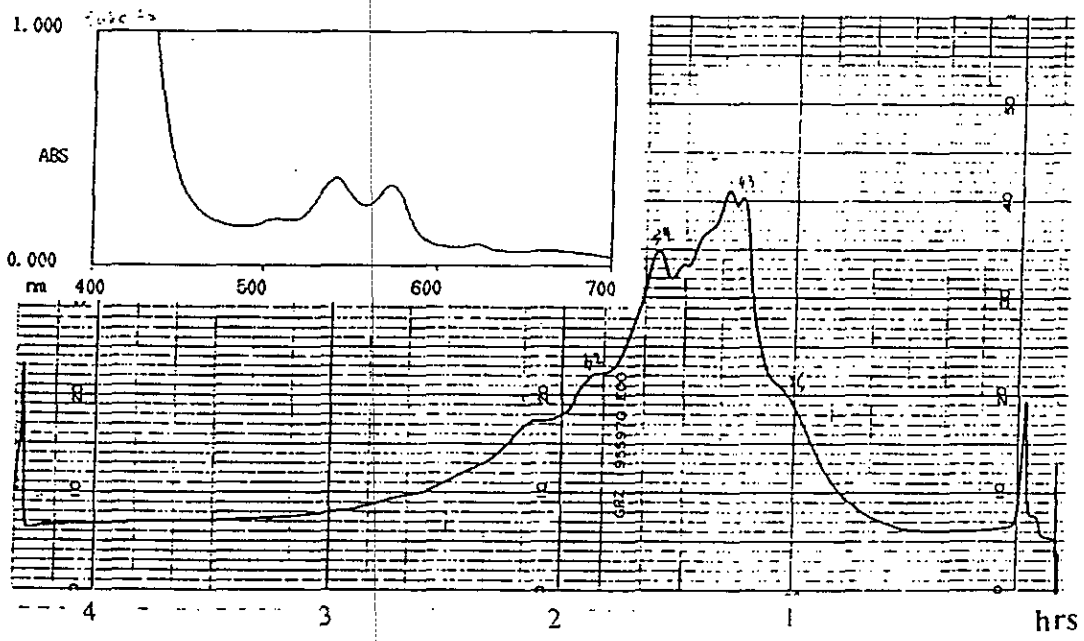

圖二 Control Hb Pkk233-2 細胞抽出物經 Resourse S 陽離子交換層析所得之分離曲線圖。左上方插圖是經 Resourse S 管柱溶離出來的 Peak 之 Visible spectrum。從波長 400→700 nm 之結果。

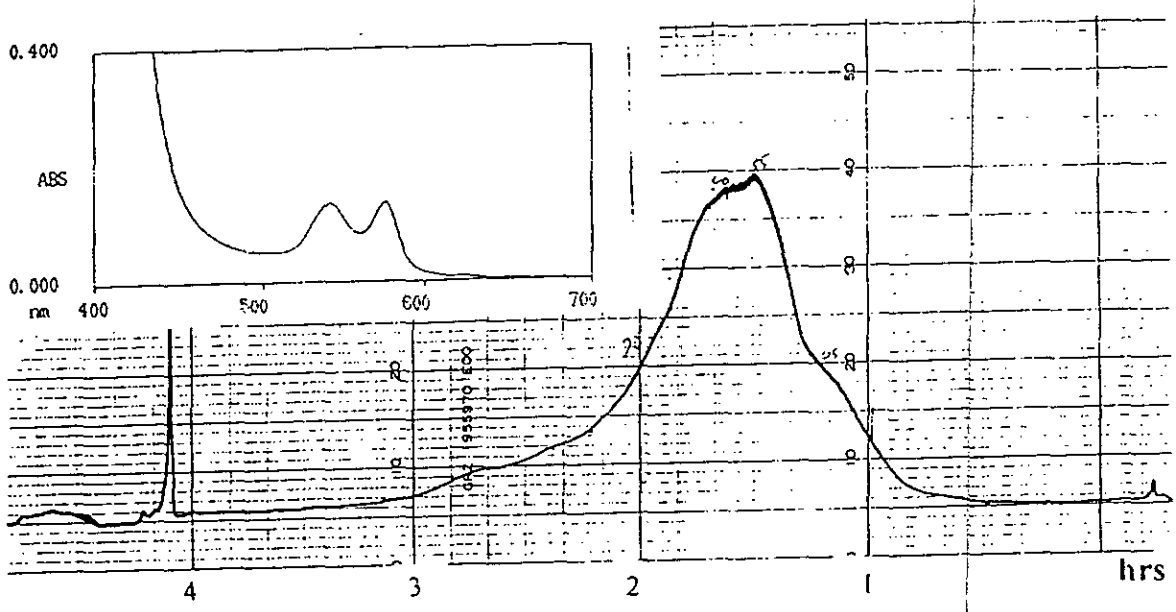

圖三 Control Hb A pET29 細胞抽出物經 Resourse S 陽離子交換層析所得之分離曲線圖。左上方插圖是經 Resourse S 管柱溶離出來的 Peak 之 Visible spectrum,從波長 400→700 nm 之結果。

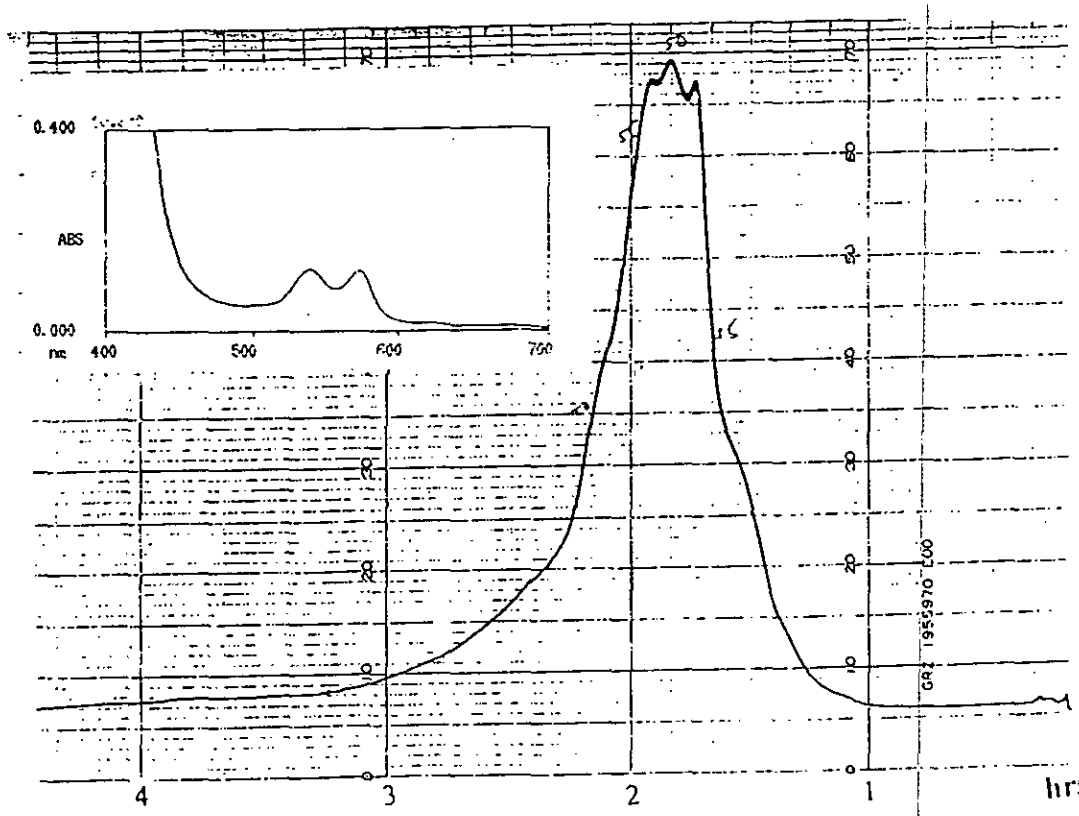

圖四 Control Hb A pQE60 細胞抽出物經 Resourse S 陽離子交換層析所得之分離曲線圖。左上方插圖是經 Resourse S 管柱溶離出來的 Peak 之 Visible spectrum。從波長 400→700 nm 之結果。

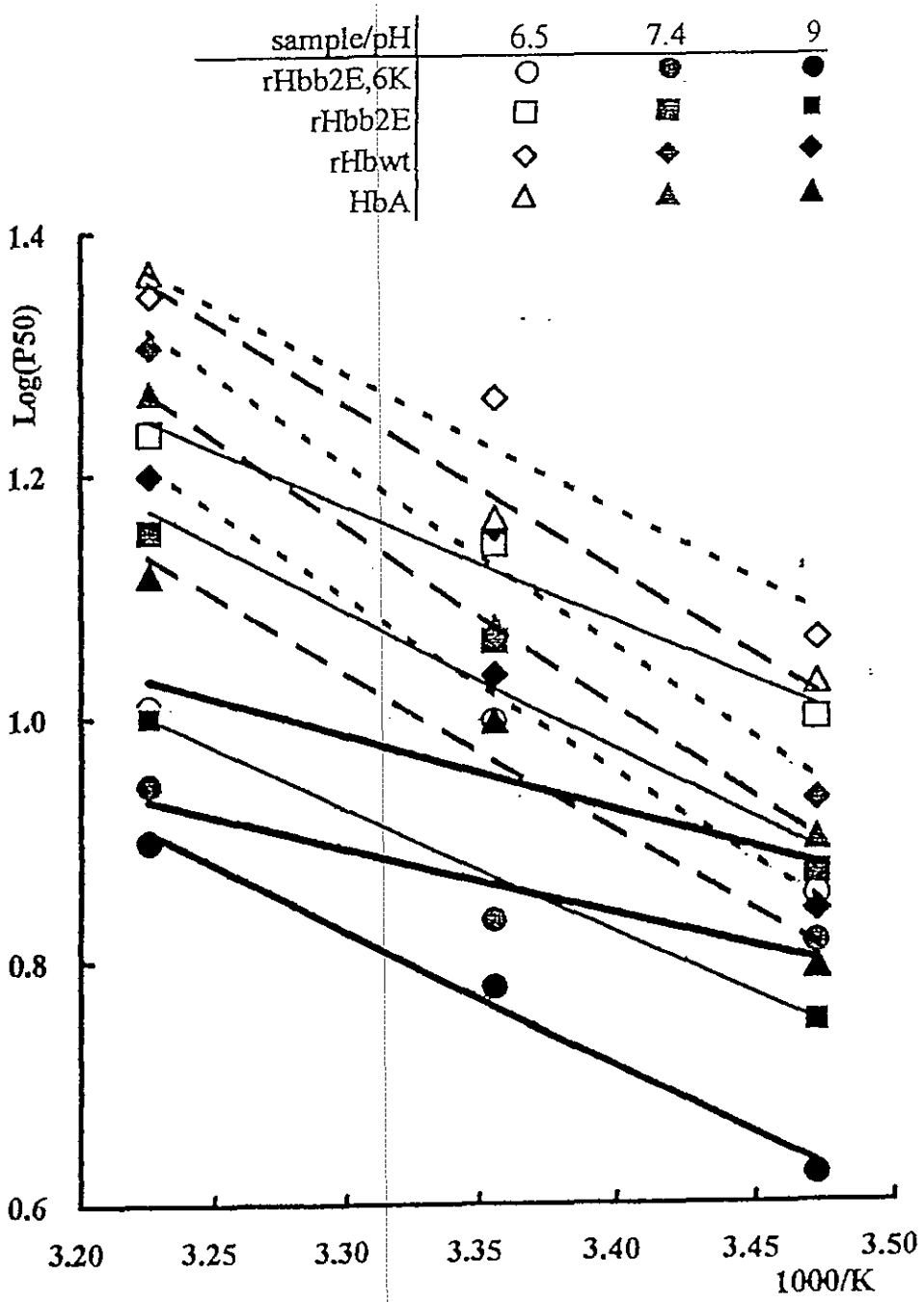

圖五、氧氣平衡曲線:溫度對血紅蛋白之影響

於 pH 6.5， pH 7.4， pH 9.0 時， P_{50} 與溫度之關係。

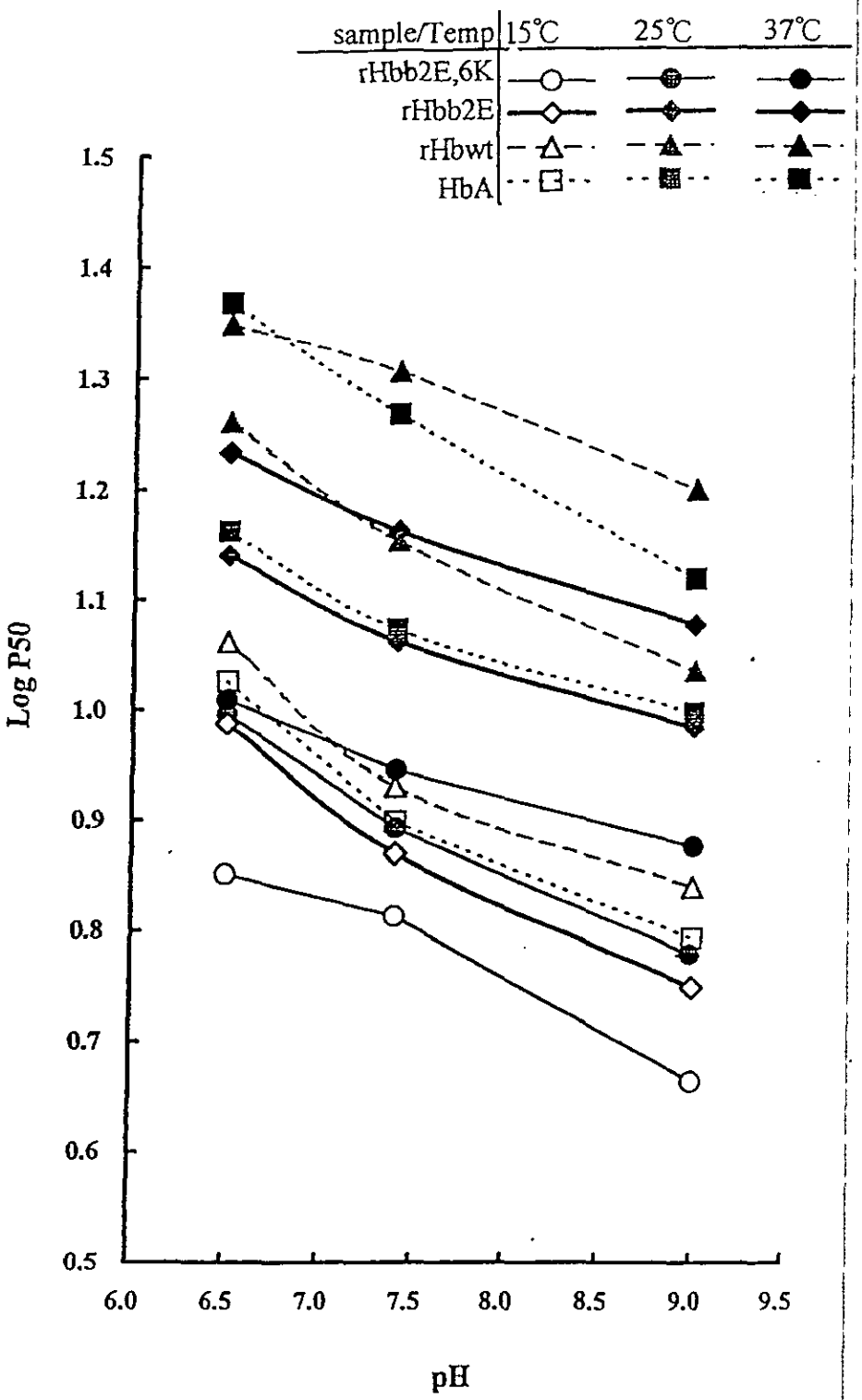

圖六、氧氣平衡曲線: pH 值對血紅蛋白之影響

於 15℃，25℃，37℃ 時 P_{50} 與 pH 之關係

Automated O_2 Equilibruim Analyzer

Automated O_2 Equilibrium Analyzr 爲一套具有高效率及準確性的氧合分析系統（見附表一），整個系統主分爲兩大主軸：

（一）硬體部份：藉由設計具溫控及 magnetic stir 的小量（1.5ml）樣品載體，減短氧合平衡時間，以得到較小量、快速精確之實驗測定。

（二）軟體部份：

利用在個人電腦上執行之 Chart for windows 程式軟體將實驗原始資料直接收集，再藉由 hemoglobin oxygenation Equilibrium 程式作進一步的分析，說明如下。

Hemoglobin Oxygenation Work（HOW） program 可分爲三部份

1.Manunal Data Processing:將"Automated O_2 Equilibrium Analyzer"system 所收集到的 Chart Text File 轉變成 A Files（PO_2,ABS）

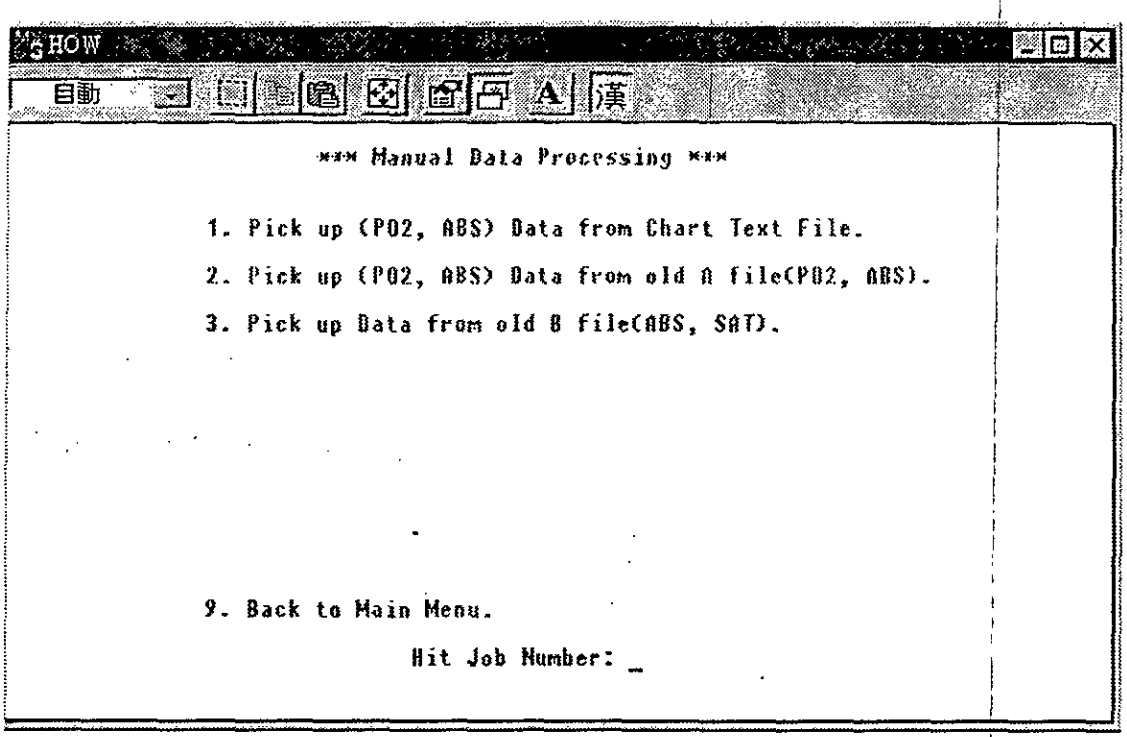

2.Grapic Data Processing:將 A Files（PO2,ABS）轉變爲 B Files（PO2,Y）格式，以進一步作 Y versus log P plot ,Hill Plot,Scatchard plot,以及 Watari & Isogai

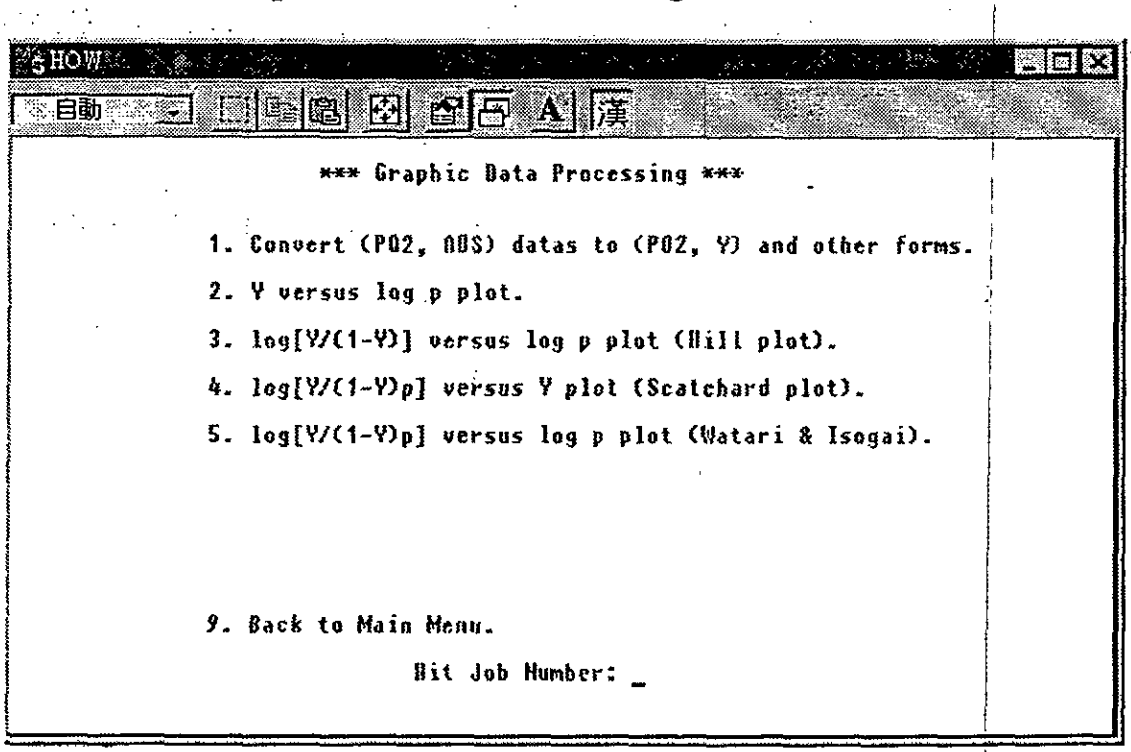

3.Adair Analysis :將經 Graphic Data Processing 處理過之 B Files 格式資料進行 Adair Analysis，可得到 K1,K4,(K2,K3)，N_{50}，Nmax，P_{50}，Pmax 等數值。

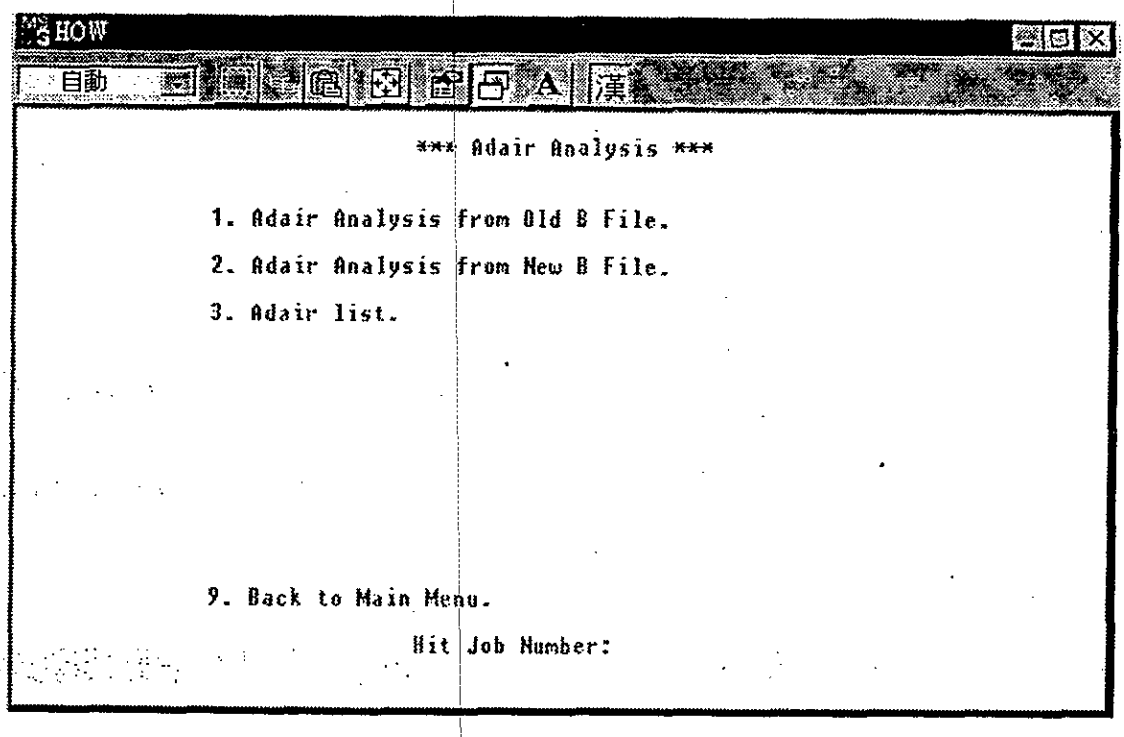

（三）結果範例

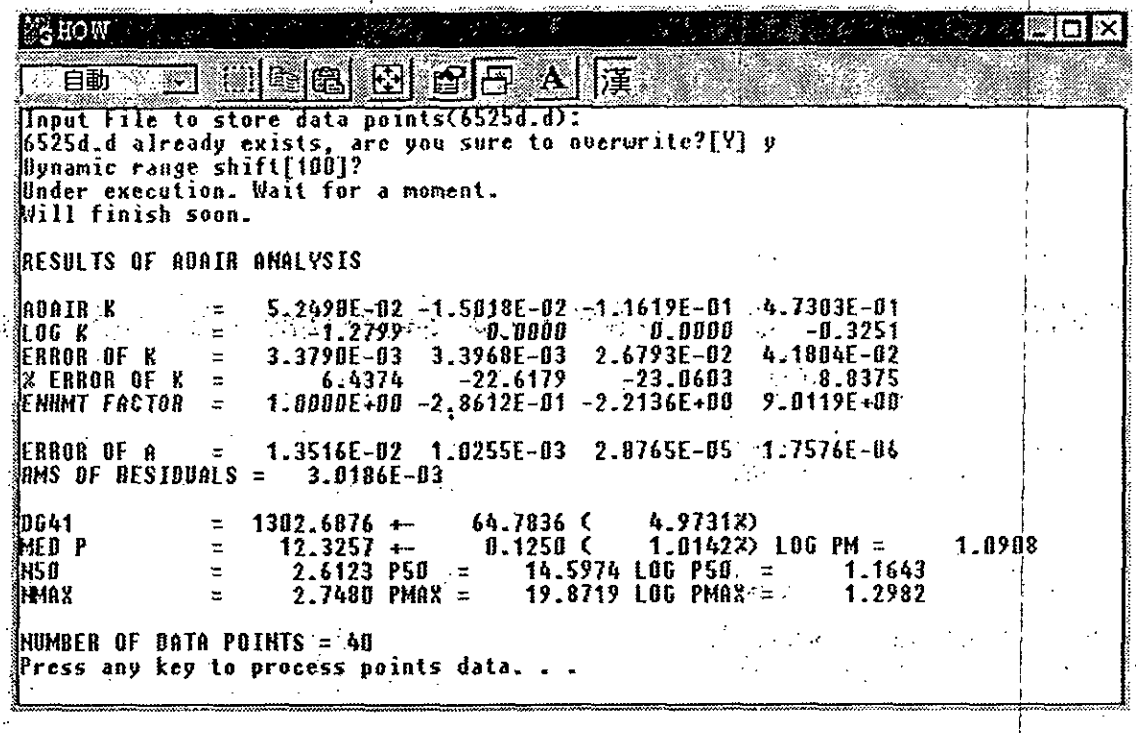
HOW
自動
Input File to store data points(6525d.d):
6525d.d already exists, are you sure to overwrite?[Y] y
Dynamic range shift[100]?
Under execution. Wait for a moment.
Will finish soon.
RESULTS OF ADAIR ANALYSIS
ADAIR K = 5.2498E-02 -1.5018E-02 -1.1619E-01 4.7303E-01
LOG K = -1.2799 -0.0000 0.0000 -0.3251
ERROR OF K = 3.3790E-03 3.3968E-03 2.6793E-02 4.1804E-02
% ERROR OF K = 6.4374 -22.6179 -23.0603 8.8375
ENHMT FACTOR = 1.0000E+00 -2.8612E-01 -2.2136E+00 9.0119E+00
ERROR OF A = 1.3516E-02 1.0255E-03 2.8765E-05 1.7576E-06
RMS OF RESIDUALS = 3.0186E-03
DG41 = 1302.6876 +- 64.7836 (4.9731%)
MED P = 12.3257 +- 0.1250 (1.0142%) LOG PM = 1.0908
N50 = 2.6123 P50 = 14.5974 LOG P50 = 1.1643
NMAX = 2.7480 PMAX = 19.8719 LOG PMAX = 1.2982
NUMBER OF DATA POINTS = 40
Press any key to process points data. . .

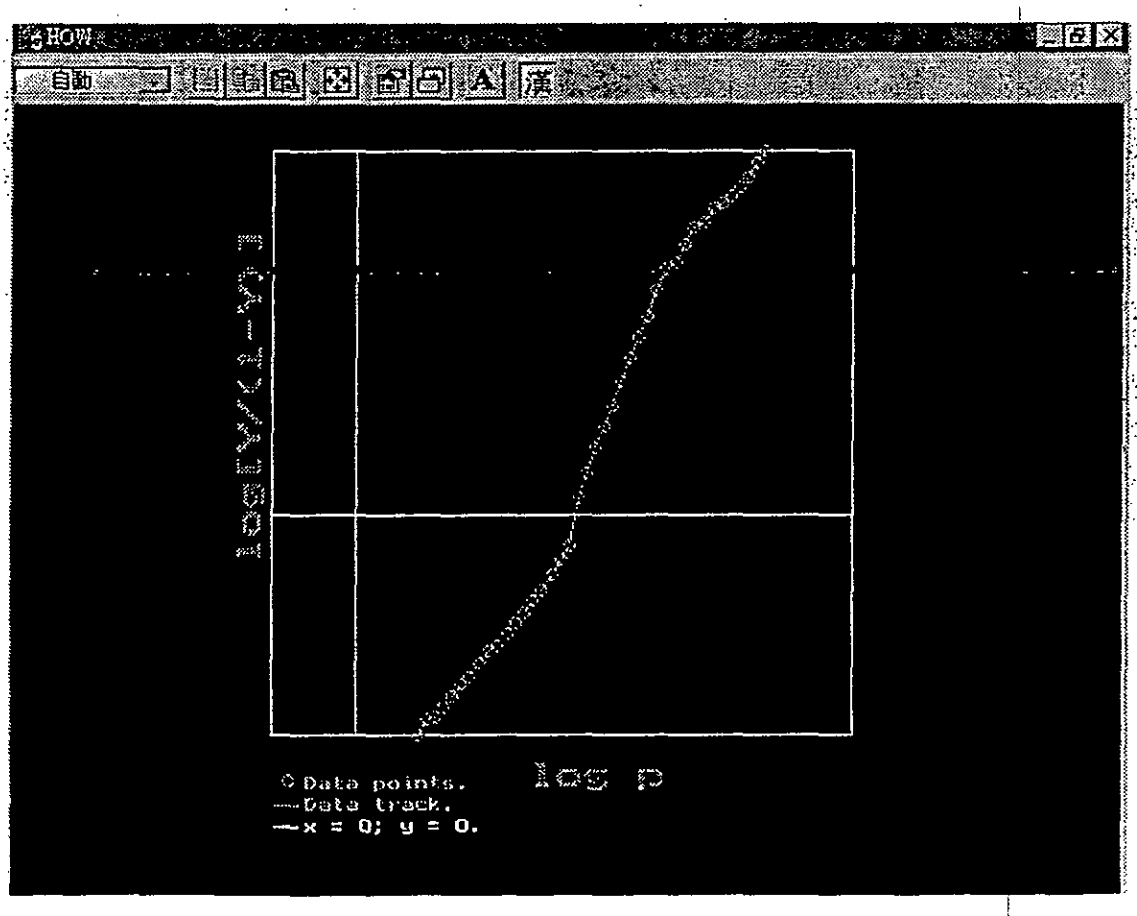
HOW
自動
log(V/(1-V))
log p
o Data points.
—Data track.
—x = 0; y = 0.

附表一、Automated O2 Equilibrium Analyzer system

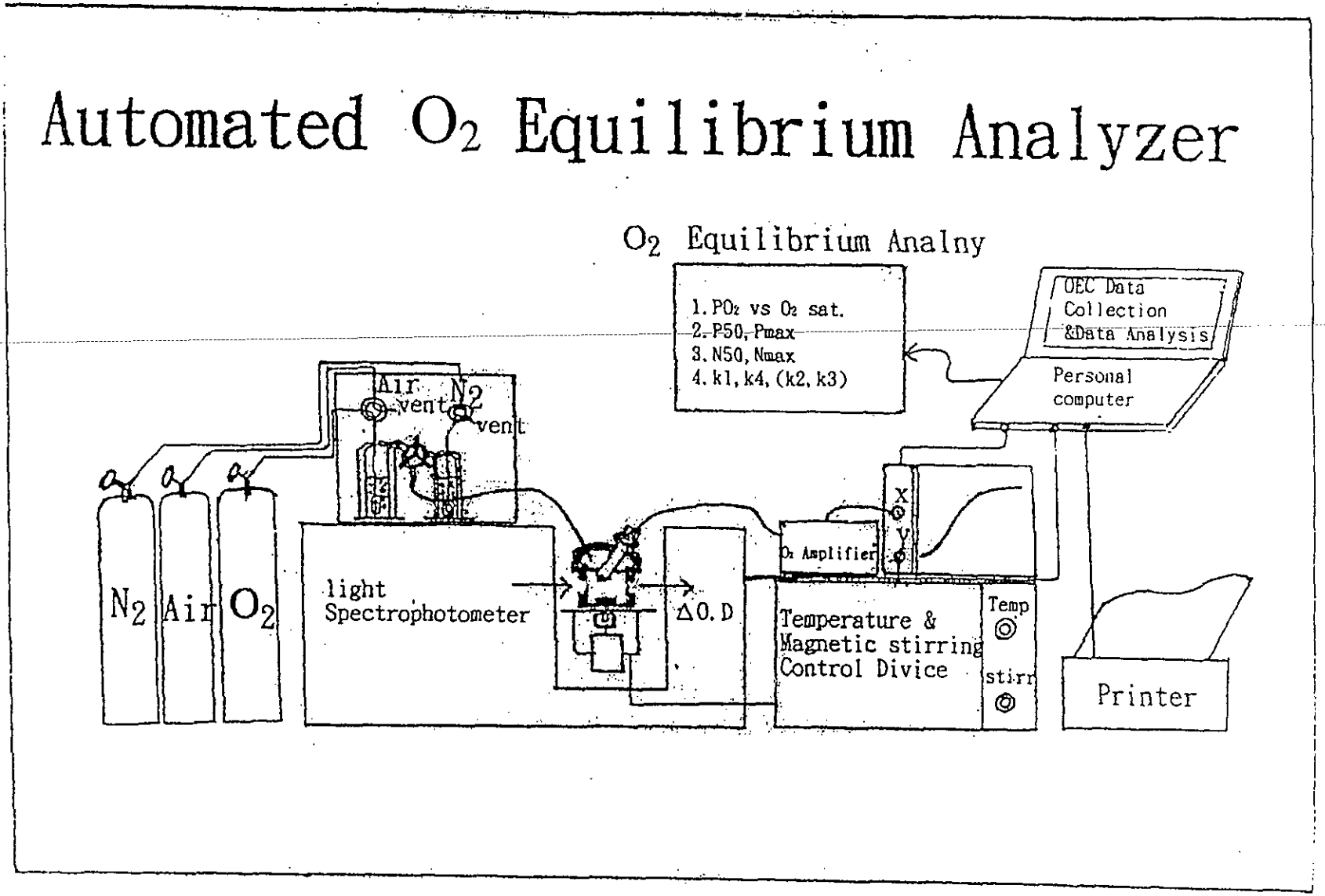

THE JOURNAL OF BIOLOGICAL CHEMISTRY
Vol. 274, No. 13, Issue of March 26, pp. 8686–8693, 1999
Printed in U.S.A.

Altered Ligand Rebinding Kinetics Due to Distal-side Effects in Hemoglobin Chico (Lys$^{\beta 66}$(E10) → Thr)*

(Received for publication, August 3, 1998, and in revised form, November 23, 1998)

Celia Bonaventura‡§, Joseph Bonaventura‡, Daniel Tzu-bi Shih¶, E. Timothy Iben‖, and Joel Friedman**

*From the ‡Duke University Marine/Freshwater Biomedical Center, School of the Environment/Marine Laboratory, Beaufort, North Carolina 28516, the ¶Institute of Cell and Molecular Biology, TMC, 250 Wu-Hsing Street, Taipei 110, Taiwan, Republic of China, ‖IBM, San Jose, California 95193, and the **Department of Physiology and Biophysics, Albert Einstein College of Medicine, Bronx, New York 10461*

Hb Chico is an unusual human hemoglobin variant that has lowered oxygen affinity, but unaltered cooperativity and anion sensitivity. Previous studies showed these features to be associated with distal-side heme pocket alterations that confer increased structural rigidity on the molecule and that increase water content in the β-chain heme pocket. We report here that the extent of nanosecond geminate rebinding of oxygen to the variant and its isolated β-chains is appreciably decreased. Structural alterations in this variant decrease its oxygen recombination rates without significantly altering rates of migration out of the heme pocket. Data analysis indicates that one or more barriers that impede rebinding of oxygen from docking sites in the heme pocket are increased, with less consequence for CO rebinding. Resonance Raman spectra show no significant alterations in spectral regions sensitive to interactions between the heme iron and the proximal histidine residue, confirming that the functional differences in the variant are due to distal-side heme pocket alterations. These effects are discussed in the context of a schematic representation of heme pocket wells and barriers that could aid the design of novel hemoglobins with altered ligand affinity without loss of the normal allosteric responses that facilitate unloading of oxygen to respiring tissues.

Exquisite molecular adaptations match the hemoglobins of widely diverse organisms to their respective physiological needs and environments. As a model protein and paradigm of allosteric control mechanisms, Hb continues to provide investigators with information on how proteins control and modify the properties of active-site metals. Studies of normal and variant human hemoglobins and model heme compounds have shown that various combinations of electronic and steric factors can alter the ligand-binding affinity of the heme iron (1–5). Our recent studies demonstrated that it was possible to differentiate electronic from steric effects by comparing oxidation curves of various types and states of Hb with oxygenation curves under the same conditions (6). Such studies led us to conclude that the extent and frequency of conformational fluctuations play a significant role in the anionic modulation of oxygen affinity of T-state Hb, with increased steric hindrance and lower affinity associated with greater structural rigidity (7).

This study further characterizes the functional consequences of changes in the heme pocket of Hb Chico (Lys$^{\beta 66}$(E10) → Thr), a naturally occurring, low-affinity Hb variant that has an increased rate of autoxidation (8). The partial pressure of oxygen required for half-saturation of Hb Chico is approximately twice that required for Hb A_0. The oxygen affinity of isolated β-chains of Hb Chico is similarly lowered relative to normal β-chains. These equilibrium properties are mirrored by changes in the transient kinetics of both ligand binding and ligand dissociation. The CO binding rates for Hb Chico in the millisecond time region are about half those for Hb A_0, and oxygen dissociation occurs about twice as fast (9).

Increased structural rigidity of residues in the heme pocket was invoked as part of the explanation for the fact that the *entire* oxygen-binding curve of Hb Chico is shifted toward lower affinity. The structure-function changes in this protein lower the ligand affinity of both its low-affinity (T-state) and high-affinity (R-state) conformations without loss of cooperativity or anion sensitivity. The substitution of Lys with Thr at position β66 was inferred to result in increased structural rigidity on the distal side of the heme pocket as a result of hydrogen bonding between the distal histidine of the β-chains and Thr$^{\beta 66}$(E10) through a bridging water molecule. This interaction would also be expected to reduce any ligand-stabilizing effects associated with hydrogen bonding between the distal histidine and bound oxygen, although the extent to which hydrogen bonding stabilizes bound ligands in the β-chain of Hb A_0 is still debated. Lowered oxygen affinity is observed for both isolated β-chains of Hb Chico and Hb Chico tetramers, indicating that this functional change has a tertiary basis apart from any alteration of the normal quaternary equilibrium between the R- and T-states (9).

The conserved distal His(E7) residue, with which Thr$^{\beta 66}$ in Hb Chico interacts, has long been considered a candidate for the modulation of oxygen affinity. Its functional role has been experimentally tested (for recent reviews, see Refs. 10 and 11). In myoglobin (Mb)[1] and in the α-chains of Hb A_0, this histidine contributes to increased oxygen affinity by stabilizing the heme-bound oxygen through either direct hydrogen bonding or polar interactions with the oxygen. The distal histidine can also play a role in controlling ligand access to the heme by participating in the control of fluctuations that result in an open and accessible pocket (10, 12–14). It can also modulate the occu-

* This work was supported by National Institutes of Health Grants ESO1908 and ESO4287 (to C. B.), a grant from the Tobacco Institute (to C. B.), and National Institutes of Health Grants HL5108 and HL58247 to J. F.). The costs of publication of this article were defrayed in part by the payment of page charges. This article must therefore be hereby marked "*advertisement*" in accordance with 18 U.S.C. Section 1734 solely to indicate this fact.

§ To whom correspondence should be addressed. Tel.: 252-504-7591; Fax: 252-504-7648; E-mail: bona@mail.duke.edu.

[1] The abbreviation used is: Mb, myoglobin.

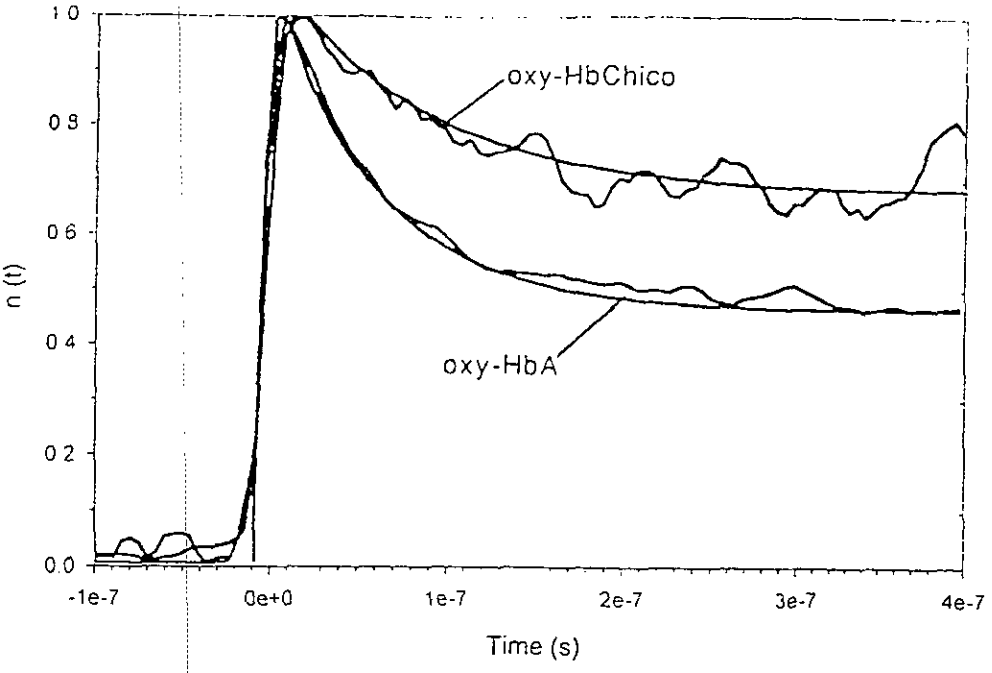

FIG. 1. Time courses of recombination after photolysis of oxy forms of Hb A and Hb Chico. The fraction of surviving unbound ligands *versus* time, n(*t*), is shown following photolysis by a laser with a pulse width of ~8 ns for the oxy forms of Hb A and Hb Chico. An excimer-pumped dye laser tuned to 540 nm was used to photodissociate the samples, and a continuous wave helium-cadmium ion laser at 441.6 nm was used as a monitor beam. The signals were normalized to their respective values at 8 ns by dividing the change in optical absorption from the pre-photolysis value by the change measured at 8 ns. See "Experimental Procedures" for further details.

ancy of the distal pocket with respect to water molecules (15). It has been shown that the presence or absence of water can influence the polarity within the heme pocket, which also influences the stability of the bound oxygen (15, 16).

This report describes the results of a further exploration of the functional properties of Hb Chico and its isolated β-chains by the techniques of resonance Raman spectroscopy and nanosecond laser photolysis followed by ligand recombination. These techniques allowed us to show that one or more heme pocket barriers in Hb Chico are increased. As a consequence of this change, in both intact Hb Chico and its isolated β-chains, the fraction of oxygen that rebinds from within the heme pocket after a nanosecond flash (geminate recombination) is significantly diminished relative to Hb A_0 and normal human β-chains. Analysis of the geminate rebinding kinetics following laser flash photolysis allowed us to quantify the magnitude of differences in O_2 and CO rebinding shown by the Hb variant and to suggest where the mutation exerts its influence along the reaction coordinate for ligand rebinding.

EXPERIMENTAL PROCEDURES

Whole blood from which Hb Chico was isolated was obtained from members of the affected family. Hb Chico and Hb A_0 were prepared and stripped of residual anions, particularly phosphates, as described previously (9). Hemoglobin concentrations were determined spectrophotometrically (17). Isolation of the β-chains of Hb A_0 and Hb Chico was accomplished with the method described by Geraci *et al.* (18). Regeneration of the β SH-chains was assured by carrying out spectrophotometric titrations of the regenerated sulfhydryl groups as described by Boyer *et al.* (19). Samples were stored in the CO form and packed in ice (0 °C) prior to the analyses reported here. Sodium dithionite (Merck) at a concentration of ~0.5% was used to deoxygenate samples prior to kinetic and resonance Raman experiments with the CO derivative. The oxygenated forms were prepared at room temperature by bubbling the HbCO samples with air while illuminating them with light whose IR spectrum was filtered out.

An excimer-pumped dye laser (Lambda Physics) was used both in the photolysis experiments (as a photodissociation light source) and in the resonance Raman experiments. The laser was operated at 50 Hz and yielded 30 milliwatts of light at 430 nm with an 8-ns pulse (full-width at half-maximum). The laser passed through a prism assembly to remove any amplified stimulated emission or fluorescence. This light beam was focused onto the sample with a spot size of ~1 × 3 mm. To avoid heating the sample and to present a fresh spot for each laser pulse, the samples were placed in a rotating quartz cell. The Raman scattering experiments were set up with back-scattering geometry. A holographic grating filter placed between a 2-inch diameter f3 collection lens and a 2-inch diameter f8 focusing lens removed unwanted laser scattering from entering the spectrometer. The reflected light was dispersed and detected by a 1.5-m single spectrograph upon whose exit slit was mounted an intensified diode array detector (750 diodes, Princeton Instruments IR4). Wavelength calibration was done with the known lines of an argon lamp. The spectral response of the system was ~3 cm^{-1}.

For the transient absorption experiments, the Hb concentrations were all between 100 and 250 μM in heme and were loaded into a 0.75-mm thick quartz cell. An excimer-pumped dye laser tuned to 540 nm was used to photodissociate the samples, and a continuous wave helium-cadmium ion laser at 441.6 nm was used as a monitor beam. A green-reflecting, blue-transmitting dichroic window was used to reflect the excitation pulse onto the sample and to allow the monitor beam to pass through co-linearly. A low-resolution spectrometer (~5-nm full-width at half-maximum) was placed in front of the detection photomultiplier tube to remove room lights and any stray light from the photodissociation pulse. A Hamamatsu RG928 photomultiplier tube wired for high current (10-kilowatt dividers) and short pulses (0.1-microfarad capacitors) was used to detect the light. The data were collected with a 1-GHz oscilloscope (Tektronics 7104) and a digitizing camera (Tektronics DCS01). The system resolution was ~8 ns.

RESULTS

Transient Absorption Studies—Transient absorption measurements following photolysis initiated with a pulsed laser revealed functional differences between Hb A_0 and Hb Chico and their isolated β-subunits in their O_2 and CO ligand rebinding kinetics. Fig. 1 is a plot of the fraction of surviving unbound ligands *versus* time, n(*t*), following photolysis by a laser with a pulse width of ~8 ns for the oxy forms of Hb A_0 and Hb Chico. The signals were normalized to their respective values at 8 ns by dividing the change in optical absorption from the pre-photolysis value by the change measured at 8 ns. The fast process that occurs in ~100 ns is attributed to geminate rebinding of O_2 molecules that have not escaped from the heme pocket (20–22). This geminate phase is characterized by a fraction of geminately rebinding ligands (f_g) and a rate (k_g). The fraction remaining unbound beyond ~0.5 μs (f_s) is attributed to ligands that have escaped into the solvent. Fig. 2 summarizes the differences in O_2 rebinding kinetics for Hb A_0 and Hb Chico as well as for their isolated β-subunits. A consistent result is that f_g and k_g for O_2 rebinding are appreciably smaller for the Hb Chico samples. For CO rebinding, a similar but much reduced protein-specific difference is observed.

Further information can be ascertained as to the functional

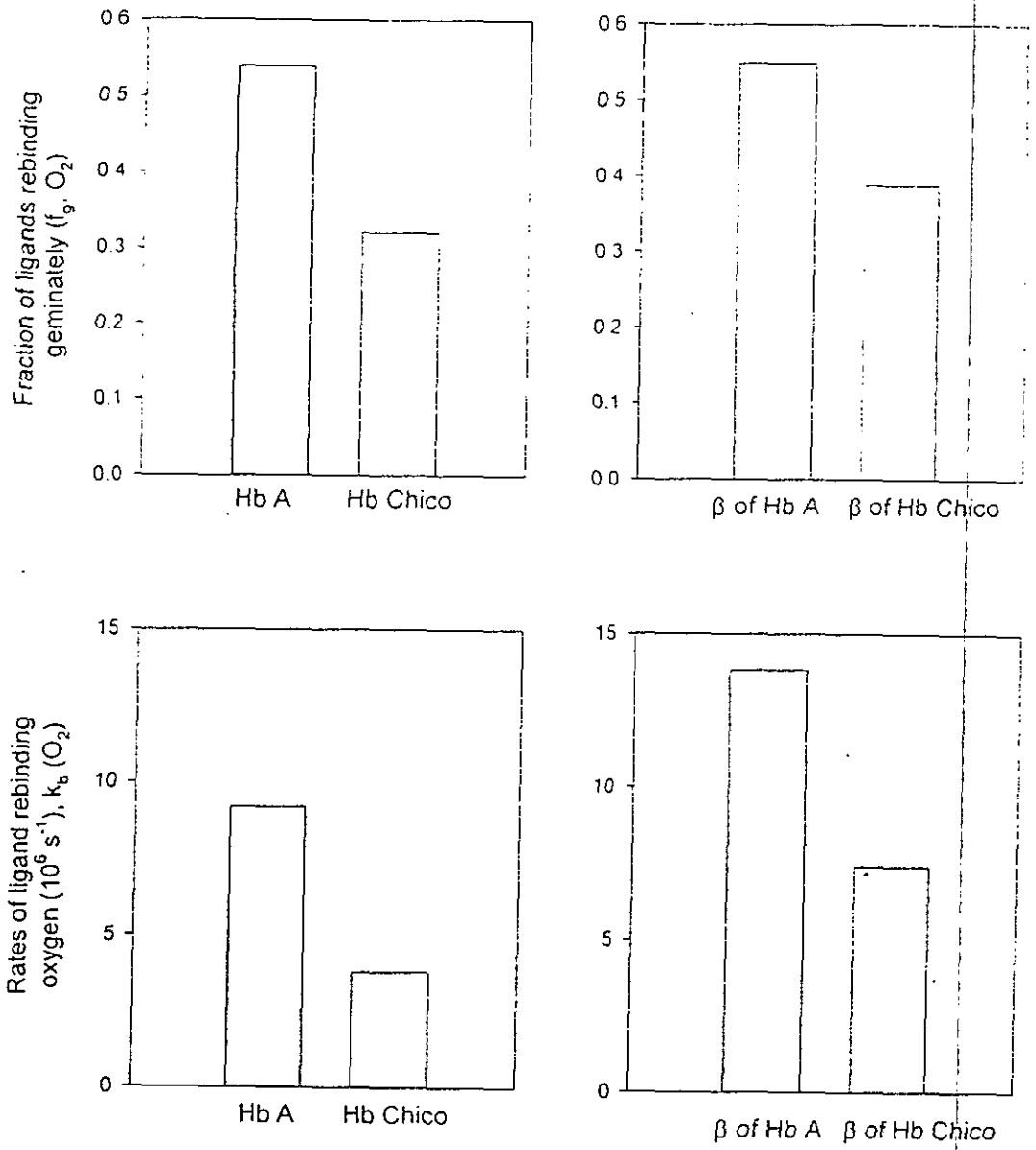

IG. 2. **Graphical representation of differences in O_2 rebinding kinetics for Hb A_0 and Hb Chico and their isolated β-subunits ıg data of Table I.**

ɪrences between Hb A_0 and Hb Chico by modeling ligand ration behavior. In the most simplified model of geminate nding, photolysis is immediately followed by an interval n the ligand occupies the distal heme pocket. From there ligand can either rebind, with rate k_b, or migrate out ard the solvent, with rate k_m. It is easily shown that the of the geminate rebinding phase (k_g) is determined by k_b + ınd that $k_b = f_g k_g$ and $k_m = f_s k_g$. These parameters are vn in Table I. In almost all cases, the values of k_m are lar for Hb Chico and Hb A_0 as well as for their subunits. O_2 escape from the heme pocket, k_m(Hb A_0)/k_m(Hb Chico) = and k_m(β of Hb A_0)/k_m(β of Hb Chico) = 0.97. CO migration of the heme pocket is also largely unaffected by the ɪtitution.

contrast to the unchanged rates of ligand escape from the e pocket, the differences in k_b for O_2 rebinding are appre-le, with k_b(Hb A_0)/k_b(Hb Chico) = 2.4 and k_b(β of Hb A_0)/ of Hb Chico) = 1.9. Similar but much smaller differences , for CO rebinding are also apparent. Thus, the structural rences between Hb Chico and Hb A_0 result in barrier ıases that affect the rate of oxygen rebinding to the active rather than migration out of the heme pocket. The small rence between samples of Hb A_0 and Hb Chico for CO ıding from the heme pocket must be reconciled to the fact

TABLE I

Fraction of ligands rebinding geminately (f_g) or escaping to the solvent (f_s), the rate of binding (k_b) or migrating out of the heme pocket (k_m), and the observed germinate rate (k_g)

Sample	Ligand	f_g	f_s	k_g	k_b	k_m
				10^7 s^{-1}	10^6 s^{-1}	10^6 s^{-1}
Hb Chico	O_2	0.32	0.68	1.2	3.8	8.1
Hb A	O_2	0.54	0.46	1.7	9.2	7.8
Hb Chico	CO	0.26	0.74	1.2	3.1	8.9
Hb A	CO	0.29	0.71	1.5	4.4	10.7
β-Hb Chico	CO	0.10	0.90	0.6	0.6	5.4
β-Hb A	CO	0.13	0.87	0.6	0.8	5.2
β-Hb Chico	O_2	0.39	0.61	1.9	7.4	11.6
β-Hb A	O_2	0.55	0.45	2.5	13.8	11.3

that the slower solution-phase CO binding to R-state Hb Chico and its isolated β-chains is half as fast as for Hb A_0 and normal β-chains (see "Discussion").

Resonance Raman Studies—To better understand the structural causes of the lowered ligand-binding affinity for Hb Chico *versus* Hb A_0, resonance Raman spectra were obtained from the same protein-ligand systems as discussed above. The probe wavelength of 430 nm couples to the $\pi\pi^*$ Soret absorption band of the heme (23–27), resulting in resonance enhancement of several protein conformation-sensitive Raman vibrational

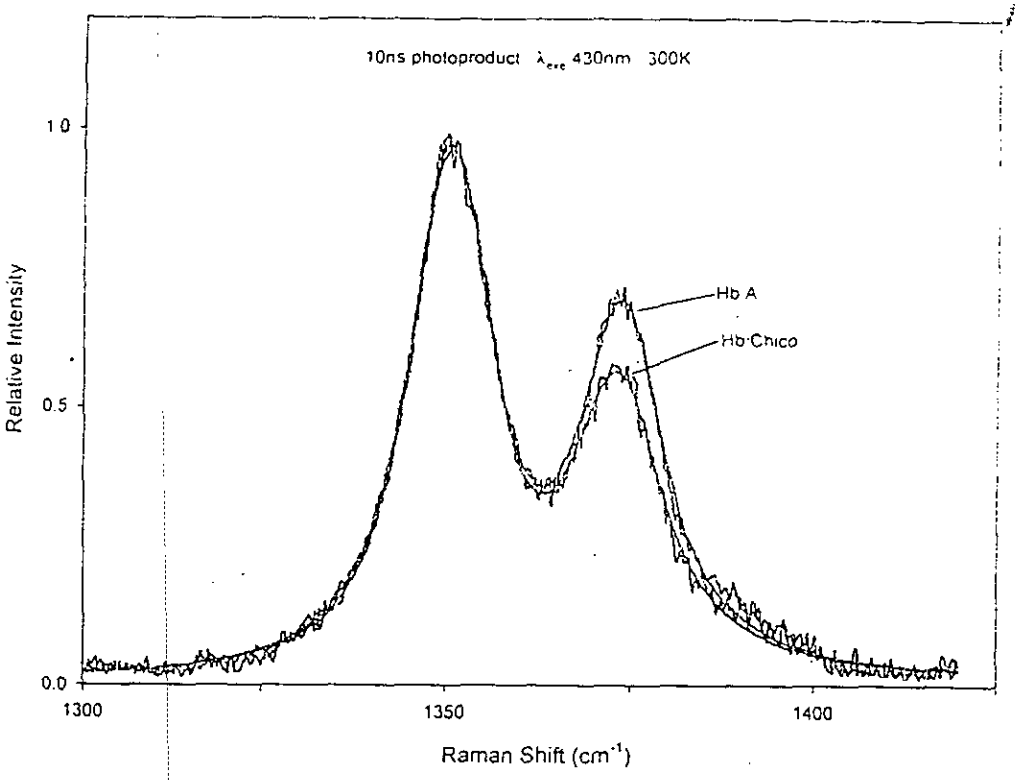

FIG. 3. Comparison of the ν4 Raman bands for partially photodissociated oxy derivatives of Hb A_0 and Hb Chico. The lower and higher frequency bands correspond to the five-coordinate oxy photoproduct and the six-coordinate unphotolyzed oxy species, respectively. The spectra were generated from identical concentrations of protein and identical excitation conditions. They are normalized with respect to the photoproduct peaks at ~1312 cm^{-1}.

bands associated with the heme and the linkage between the heme and the proximal histidine. We focused on two bands: 1) the porphyrin band labeled ν4 (1350–1385 cm^{-1}) (24) and 2) the iron–proximal histidine band, ν(Fe-His) (200–240 cm^{-1}) (26, 27). The ν4 band involves a symmetric vibrational breathing mode of the porphyrin made up largely of C–N stretches. It is very sensitive to changes in heme ligation. For liganded ferrous Hb, ν4 is ~1374 cm^{-1}, whereas for deoxy-Hb and photolyzed Hb, ν4 is ~1352 cm^{-1}. The frequency of ν4 for the five-coordinate species is sensitive to both quaternary and tertiary structure of hemoglobins (27). Fig. 3 shows ν4 for HbO_2 A_0 and HbO_2 Chico photolyzed and probed with a 10-ns laser pulse at 430 nm (50 Hz, 30 milliwatts). The band at ~1356 cm^{-1} is characteristic of photolyzed Hb, whereas the band at ~1376 cm^{-1} is characteristic of either liganded or methemoglobin. The absorption spectrum indicates that there is no measurable met formation in these samples. The fractional integrated area of the 1376 cm^{-1} band was found to be 0.8 for HbO_2 A_0 and 0.7 for HbO_2 Chico. For deoxy forms, no band at ~1375 cm^{-1} was detected, whereas for the easily photodissociated carboxy forms, the 1375 cm^{-1} band was significantly decreased, indicative of nearly complete photodissociation.

The difference in fractional intensity of the 1356/1375 cm^{-1} band between HbO_2 Chico and HbO_2 A_0 (for samples having the same optical density) means that it is harder to photodissociate the latter. This difference in the ease of photodissociation with an 8-ns pulse suggests that there is either a subnanosecond geminate phase for which Hb A_0 has a higher geminate yield or that the actual intrinsic quantum yield for photodissociation is lower for Hb A_0. Future studies are planned to examine this effect.

The ν(Fe-His) bands for the deoxy forms as well as the photoproducts of the carboxy and oxy forms of Hb A_0 and Hb Chico were measured. The frequency of the ν band is very sensitive to structural changes on the proximal side of the heme that have been shown to correlate with ligand affinities (26–29). No discernible differences in ν(Fe-His) could be detected between the Hb Chico structures and those measured or reported for Hb A_0 (28, 30).

DISCUSSION

The objective of this study was to determine the nature and origin of consequences for ligand binding and dissociation within the heme pocket that result from the point mutation that causes Hb Chico to have dramatically lowered ligand affinity in both low-affinity (T-state) and high-affinity (R-state) conformations. The nanosecond geminate rebinding experiments showed that one or more heme pocket barriers to rebinding of oxygen are indeed increased in Hb Chico and in its isolated β-chains. Knowledge of the site at which the mutation has occurred and the existing x-ray crystallographic data implicate tertiary-level changes on the distal side of the heme as the source of the modified ligand reactivity. This view is further strengthened by the Raman data that indicate that the structural parameters associated with the proximal side of the heme are the same in Hb A_0 and Hb Chico. The question remains as to where along the reaction coordinate for ligand binding the distal pocket perturbation in Hb Chico exerts its influence. To address that question, we must consider the protein- and ligand-specific pattern of changes observed in the geminate recombination process.

The process of geminate recombination provides a direct window into the molecular events that shape ligand dynamics within the local environment of the heme. Geminate recombination at room temperature was first reported for nanosecond time-resolved absorption (20, 21) and Raman spectroscopy (22). These studies revealed that the quantum yield for photodissociation of the CO forms of Hb and Mb differ due to a 100-ns geminate rebinding process that is more pronounced in Hb.

Many workers, starting with Frauenfelder and co-workers (31), have contributed to our understanding of the barriers to ligand binding and dissociation. Recent room-temperature studies provide convincing evidence for there being spatially distinct regions from which geminate recombination can occur (32–35). Subsequent to photodissociation, ligand diffusion occurs in the progressive spatial separation of the ligand and heme. In Mb, the ligand, still within the heme pocket, can occupy accessible cavities or docking sites; and geminate rebinding from these sites gives rise to different geminate rebind-

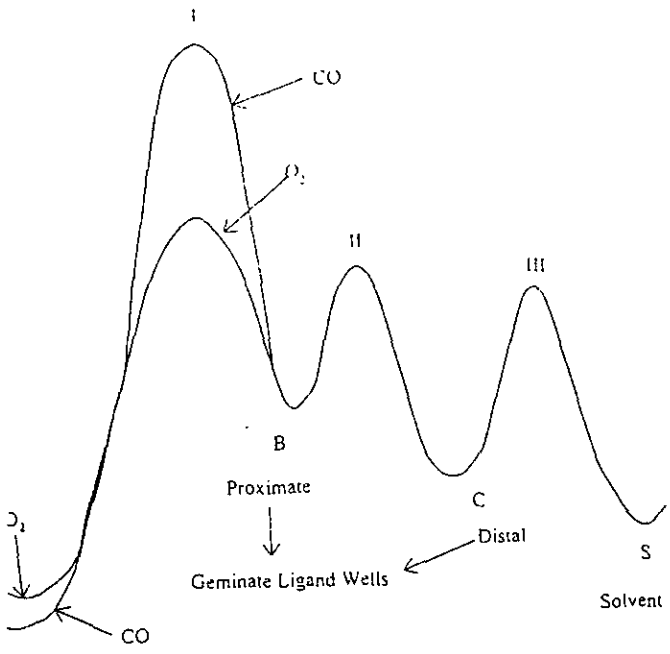

FIG. 4. **Reaction-coordinate diagram for ligand dissociation d recombination in Hb.** This qualitative energy coordinate dia- m illustrates barrier differences for O_2 and CO ligands as described der "Discussion." Proximate and distal geminate wells refer to the ne pocket sites occupied by the dissociated ligand that are kinetically th respect to rebinding) close to or far from the heme iron, respectively.

g phase(s). Scott and Gibson (35) have shown that xenon ms can alter the pattern but not the yield of geminate binding by occupying, and thereby blocking access to, cavities thin the distal pocket of Mb.

A reaction-coordinate diagram for three spatially separated me pocket barriers is shown in Fig. 4. The potential energy of ell A represents the condition for the iron-bound ligand. ells B and C correspond to the potential energy wells for the gand as it moves from a position very close to the heme (the oximate well) to more distant regions of the heme pocket (the stal well). S represents the ligand in the solvent. The poten- al energy of Barrier I controls iron–ligand bond formation. arrier II controls the ligand motion between the site of iron– gand bond formation and transient docking sites on the distal de, spatially removed from the iron. Barrier III regulates gand escape from the heme pocket into the bulk solvent. It is kely that Process 1, B → A, can be further subdivided since binding processes occurring from about one to several hun- red picoseconds have been observed. However complex the nderlying reality, many ligand- and protein-specific processes ithin the heme pocket can be compared within the context of his reaction-coordinate diagram and the associated kinetic cheme given below.

$$A \underset{k_{ba}}{\overset{k_{ab}}{\rightleftharpoons}} B \underset{k_{cb}}{\overset{k_{bc}}{\rightleftharpoons}} C \underset{k_{sc}}{\overset{k_{cs}}{\rightleftharpoons}} S$$

SCHEME I

Considerable information has been obtained about the rela- ive potential energy barriers in the heme pocket of Hb A_0. Ligand specificity in the geminate rebinding process has shown hat Barrier I is much higher for CO compared with O_2 and NO 36–39). In Hb A_0, oxygen exhibits geminate rebinding on the ime scales of several picoseconds, hundreds of picoseconds, nd hundreds of nanoseconds, whereas CO displays negligible rebinding on subnanosecond time scales. This ligand specificity s reflected in the differences shown for O_2 and CO in Fig. 4. As a result of this ligand dependence of the inner barrier, on-rates for oxygen and especially NO binding can approach the diffusion limit, whereas CO binding is slower (40). Similarly, the lower yield of geminate recombination for CO relative to O_2 is understandable in terms of a higher Barrier I for CO.

Friedman and co-workers (28, 41, 42) presented a mechanistic explanation for the origin of this ligand-specific barrier-height difference based upon differences in the nature of the transition state for CO and O_2. The claim is that CO requires a nearly planar heme transition state, whereas oxygen can form a bond with the heme when the iron is still partially out of the heme plane. Thus, much larger fluctuations in structure are required for the formation of the CO-heme transition states. This assessment of the transition state is similar to the kinetically and thermodynamically derived conclusion of Szabo and Karplus (43) that asserts that CO has a more product-like transition state, like that when ligand is bound, whereas O_2 has a more reactant-like transition state. There is also evidence that the orientation of the CO contributes to the energy of the transition state. In particular, the picosecond IR absorption studies of Anfinrud and co-workers (44, 45) show that bond re-formation proceeds in myoglobin for an upright transition-state conformation of the photodissociated CO.

For a given ligand, the height of Barrier I is both protein- and conformation-dependent. It has been shown that in Hb A_0, the height of Barrier I is highly sensitive to both tertiary and quaternary structure (46). The geminate yield decreases as the heme pocket becomes more T-like, consistent with increases in Barrier I. The decrease in the geminate yield in these instances correlates with spectral changes that are attributed to proximal strain as reflected in Raman measurements of the iron–proximal histidine linkage (28–30, 38, 47). These proximal effects appear decoupled from distal-side effects, as seen in a study on Hb Zurich where the inositol hexaphosphate effect on the geminate rebinding of CO was found to be similar to that in Hb A_0, despite the large distal-pocket alteration created by the replacement of the distal histidine with an arginine in this Hb variant (48). A large part of the inositol hexaphosphate effect on geminate rebinding has been inferred to be due to a proximal-side effect, as indicated by the reduction in frequency of the iron–proximal histidine stretching mode in the photoproduct spectra of both HbCO A_0 and HbCO Zurich upon adding inositol hexaphosphate.

The absence of detectable shifts in ν(Fe-His) between Hb A_0 and Hb Chico for both the deoxy-T and photoproduct R forms of the protein indicates that the geminate rebinding differences do not have a proximal-strain origin. It has been argued (49) that factors that increase the rate of tertiary relaxation on the time scale of geminate rebinding can contribute to a progressive increase in Barrier I and thus decrease the geminate yield. It is therefore possible that enhanced relaxation of the initial R-state photoproduct structure in Hb Chico is responsible for the observed reactivity differences. The arguments given below that are based on differences in the distal heme pocket are, however, more plausible in this instance.

Relative heights of the other heme pocket barriers in Hb A_0 can be estimated. Picosecond studies of the geminate process with a 30-ps excitation pulse reveal that the quantum yields for the subnanosecond geminate phase for oxygen and CO are ~50 and 2%, respectively, for Hb A_0 (38, 48). This result indicates that from Well B, Barriers I and II are comparable for oxygen ($k_{ba}/k_{bc} \sim 1$). For CO, however, Barrier I is clearly much greater than Barrier II ($k_{ba}/k_{bc} \ll 1$). Since k_g, the geminate rate from Well C (but not the quantum yield), is essentially ligand-independent, the barrier controlling escape into the solvent (Barrier III) and the barrier controlling the movement of the ligand

back into Well B are, in first approximation, ligand-independent for the Hb A_0 tetramer. Rebinding of oxygen from Well B is much faster than the decay of the ligand in Well C, with the consequence that the crossing of Barrier II and ligand escape are rate-determining for the rebinding of oxygen from Well C. The geminate yield of ~50% for oxygen from Well C indicates that the heights of Barriers II and III are comparable. Thus, for O_2, $k_{ba} \gg k_{cb} \cong k_{cs}$, and the ratio k_{cb}/k_{cs} determines the nanosecond geminate yield. For CO, where the height of Barrier I is much greater than for oxygen and where the rates but not the yields for the nanosecond process are essentially independent of protein-induced changes in Barrier I, $k_{ba} \ll k_{cb} \cong k_{cs}$, and k_{ba}/k_{cs} determines the geminate yield.

The role of specific distal heme pocket residues in the partitioning of the geminate rebinding between the fast and slow phases has been documented by site-directed mutagenesis studies on Mb (10). Rebinding studies of genetically engineered mutants in conjunction with dynamic simulations for MbNO indicate that certain substitutions on the distal side can appreciably alter the heme pocket barriers. For example, the substitution Leu(B10) → Phe inhibits the motion of dissociated ligands away from the iron and simultaneously reduces access to the iron for those ligands that have successfully diffused to the most distant regions of the heme pocket (32, 34). Many aspects of the partitioning between fast and slow phases of geminate rebinding are still unclear. The possibility remains that this partitioning is controlled by tertiary conformational fluctuations and relaxations that modulate both distal- and proximal-side effects on heme ligation.

The above considerations, relative to the qualitative pictorial representation in Fig. 4 of the heme pocket barriers in Hb A_0, establish a context for discussion of the functional modifications of Hb Chico and its isolated β-chains. The previous studies of Hb Chico established that its oxygen affinity is lowered to about half that characteristic of Hb A_0. The oxygen affinity of its isolated β-chains is similarly lowered relative to normal β-chains. These equilibrium properties indicate that the well depth for bound ligand (Well A) in Hb Chico as well as its isolated β-chains is significantly decreased relative to that of Hb A_0 and normal β-chains. The equilibrium situation is mirrored by changes in the transient kinetics of both ligand binding and ligand dissociation on the millisecond time scale. The CO binding rates for Hb Chico in the millisecond time region are about half those for Hb A_0, and oxygen dissociation occurs about twice as fast (9). The decreased well depth for bound ligands contributes to the observed 2-fold increased rate of non-photoinduced dissociation of O_2 and the moderately increased rate of CO dissociation from fully liganded Hb Chico.

The structural differences between Hb Chico and Hb A_0 clearly result in increases in one or more barriers that affect the geminate rate of oxygen rebinding to the active site. This is revealed by the nanosecond geminate rebinding kinetics, where dioxygen rebinding shows a dramatic decrease. Much smaller decreases are seen in rates of CO rebinding in going from Hb A_0 to Hb Chico. This contrasts with the large decreases observed in previous millisecond time scale studies where it was shown that the binding of CO from solution shows substantial decreases for both Hb Chico and its isolated β-chains relative to Hb A_0 and its β-chains (9). To reconcile these results, we must invoke a structural change that occurs after photodissociation on a time scale longer than that of the geminate process, *i.e.* ~100 ns. We suggest that the observed reduction in CO "on"-rates in the millisecond time range can be explained based on the x-ray crystallographic structure of deoxy-Hb Chico (9). The crystal structure reveals that water is held in the distal pocket of Hb Chico and acts as a bridge between the distal histidine and Thr(E10) in the deoxy state. The binding of a ligand at the iron requires the displacement of the water to a sterically neutral site. Studies on mutant myoglobins strongly support the claim that site-stabilized waters in the distal pocket act as steric effectors that slow down the diffusion time of ligands from the solvent to the iron (15, 16, 50). It appears that water has not as yet re-entered the appropriate steric hindering site in the distal pocket of the photolyzed HbCO Chico on the time scale of the geminate process. This result suggests that CO must first move from the heme pocket before water can occupy the site between His(E7) and Thr(E10).

It can be readily seen from Table I that the isolated β-chains (as tetramers) of both Hb A_0 and Hb Chico exhibit less geminate rebinding than the corresponding $\alpha_2\beta_2$-tetramers. The effect is especially noticeable for the CO derivatives, where the β_4-tetramers show much slower rates of CO rebinding than the $\alpha_2\beta_2$-tetramers. The simplest models of Hb reactivity predict that the reactivity of the R-state tetramer should resemble that of either the isolated chains or the αβ-dimers. The limitations of this simple view were indicated by studies showing that the last available subunit in R-state $\alpha_2\beta_2$-tetramers binds ligands with higher affinity than αβ-dimers (51). This phenomenon, termed quaternary enhancement, was shown in recent studies to be evident in an increased geminate yield for fully liganded $\alpha_2\beta_2$-tetramers relative to the corresponding dimers (52). Based on geminate rebinding data and Raman spectra for the photoproducts of tetrameric and dimeric forms of Hb A_0, it was claimed that the quaternary enhancement effect arises from a proximal-heme environment in the R-state photodissociated $\alpha_2\beta_2$-tetramer that favors rebinding relative to that for αβ-dimers (29). This more favorable environment is reflected in the higher frequency of ν(Fe-His) for the photoproduct of $\alpha_2\beta_2$-tetramers compared with either αβ-dimers or isolated α- and β-chains of Hb A_0 (29, 53). A more favorable proximal environment, with lower proximal strain, translates into a lower barrier for geminate rebinding to the extent that the transition state has product-like character. Since the rebinding of CO relative to O_2 is more likely to require a transition state with an in-plane iron (28, 41, 42), it is probable that the geminate rebinding of CO is more responsive to proximal perturbations compared with O_2, which would account for the ligand-specific (CO/O_2) differences between β_4-tetramers and $\alpha_2\beta_2$-tetramers shown in Table I.

The geminate recombination experiments under consideration were initiated by excitation with a 10-ns pulse. This creates a photoproduct population that has the ligand predominantly in Well C. For a ligand to geminately recombine, it must first overcome Barrier II, followed by bond formation controlled by Barrier I. In competition with the geminate process is the escape of the ligand into the solvent as controlled by Barrier III. One explanation that would account for the pattern of change in the geminate recombination in going from Hb A_0 to Hb Chico is that the amino acid substitution in Hb Chico causes a distal-side heme pocket perturbation that increases Barrier II relative to its height in Hb A_0 for both O_2 and CO. As can be seen from Fig. 4, an increase in Barrier II would have less effect on the geminate rebinding of CO as long as k_{ba}/k_{bc} remains small, whereas the nanosecond geminate yield and the nanosecond rebinding of dioxygen should decrease and slow down, as is observed.

Although ligand-independent increases in Barrier II are sufficient to explain most of the data, some evidence points to a ligand-specific increase in Barrier I for O_2 rebinding to Hb Chico. Notably, the yield of photodissociation at 10 ns is higher for HbO_2 Chico than for HbO_2 A_0. An increase in Barrier I in Hb Chico could have this result; the apparent increase in

egree of photodissociation would result from a decrease in the umber of ligands quickly rebound. A degree of uncertainty in sing the 10-ns Raman measurement as an indication of small anges in the subnanosecond kinetics yields a less-than-rong argument for a Barrier I increase. Verification of a gand-specific increase in Barrier I in Hb Chico would require picosecond rebinding study. If Barrier I has increased, then e yield for both fast and slow geminate phases should de-ease. If Barrier II has increased without a change in Barrier then the yield for the fast-phase rebinding process should crease at the expense of slower phase rebinding, *i.e.* the ratio the quantum yield for the picosecond and nanosecond rebind-g should increase.

Recent studies on the effect of distal heme pocket polarity on e bond energies of the iron–ligand bond indicate that the ability of bound oxygen is much more sensitive to polarity fects than that of bound CO (11). If the transition state for the rmation of the iron–ligand bond shows a parallel sensitivity, ien it might be anticipated that Barrier I would also be more olarity-dependent for O_2 than for CO. If this mechanism is perative, then the significant decrease in geminate rebinding r O_2 in going from Hb A_0 to Hb Chico could arise from a more olar distal heme pocket environment in the latter, providing a ore negatively charged environment for the transition state.

more negatively charged distal pocket would also have the cpected consequence of increasing the non-photoinduced rates ligand dissociation for both CO and O_2 in going from Hb A_0 Hb Chico, as is observed (9). For oxygen, an increase in the egative charge in the vicinity of the bound oxygen would be cpected to weaken hydrogen bonding to the oxygen, which, at ast in Mb, contributes strongly to the stability of the iron–cygen bond. Similarly, an increase in negative charge near the ound CO is known to decrease the stability of bound CO, as eflected in both the Fe–C and inversely correlated CO stretch-g frequencies (54–56).

A combination of loss of hydrogen-bonding stabilization of ound ligands and the increased polarity in the heme pocket uld bring about a decrease in well depth for ligands bound to oth high- and low-affinity conformations of Hb Chico. Another echanism that could contribute to this distinct functional teration is an increased structural rigidity on the distal side the heme pocket. As noted, the substitution of Thr for Lys at osition β66, on the distal side of the heme, was inferred to sult in increased structural rigidity as a result of hydrogen nding between the distal histidine of the β-chains and $hr^{\beta 66}$(E10) through a bridging water molecule. Localized ri-dity of the Hb structure in the heme pocket region, brought out by this hydrogen bonding, could directly affect the bar-ers to oxygen rebinding. It has been shown that the distal stidine can act in conjunction with other heme pocket resi-ues to control ligand access to the heme by participating in the ntrol of fluctuations that result in an open and accessible eme pocket (10, 12–14). Accordingly, modifications that re-rict motion of the distal histidine could result in altered rriers to ligand rebinding and dissociation.

CONCLUSIONS

This study indicates that the molecular mechanism behind e altered reactivity of Hb Chico and other mutant hemoglo-ns can be dissected by use of a combination of kinetic and pectroscopic probes that can be viewed as a general scheme for alyzing ligand reactivity changes in variant hemoglobins. In rticular, the changes in the picosecond and nanosecond gem-ate phases in conjunction with ligand-specific behavior pro-de a means of determining where functional alterations occur ong the reaction coordinates for ligand rebinding. The reac-on-coordinate data in conjunction with the CO or Fe–C stretching frequency for HbCO derivative, which indicates the effective polarity of the distal pocket, can be used to implicate charge-stabilization effects. The resonance Raman spectra ex-pose changes on the proximal side of the heme pocket. A com-parison between solvent-derived ligand binding and geminate rebinding can, in addition, reflect ligand displacement of local-ized water that blocks access to the iron. Such comprehensive studies are of timely importance in that they can help in de-veloping synthetic strategies based on molecular biophysics for selectively altering ligand-binding properties of hemoglobins for pharmaceutical uses. The specific functional alterations in Hb Chico demonstrate that structural alterations in the distal heme pocket can alter ligand affinity at the tertiary level, without loss of the normal allosteric responses that facilitate oxygen unloading to respiring tissues.

Acknowledgment—We thank Dr. John Howard (Chico Medical Group of California) for the generous contribution of blood samples.

REFERENCES

1. Perutz, M. F. (1983) *Mol. Biol. Evol.* 1, 1–28
2. Traylor, T. G., Berzinis, A. P., Cannon, J. B., Campbell, D. H., Geibel, J. F., Mincey, T., Tsuchiya, S., and White, D. K. (1980) *Adv. Chem. Ser.* 191, 219–233
3. Perutz, M. F., Fermi, G., Luisi, B., Shaanan, B., and Liddington, R. C. (1987) *Acc. Chem. Res.* 20, 309–321
4. Baldwin, J. M. (1975) *Prog. Biophys. Mol. Biol.* 29, 225–320
5. Ho, C., and Russu, I. M. (1987) *Biochemistry* 26, 6299–6305
6. Faulkner, K. M., Bonaventura, C., and Crumbliss, A. L. (1994) *Inorg. Chim. Acta* 226, 187–194
7. Bonaventura, C., Tesh, S., Faulkner, K. M., Kraiter, D., and Crumbliss, A. L. (1998) *Biochemistry* 37, 496–506
8. Shih, D. T.-b., Perutz, M. F., Gronenborn, A. M., and Clore, G. M. (1987) *J. Mol. Biol.* 195, 453–455
9. Bonaventura, C., Cashon, R., Bonaventura, J., Perutz, M., Fermi, G., and Shih, D. T.-b. (1991) *J. Biol. Chem.* 266, 23033–23040
10. Olson, J. S., and Phillips, G. N., Jr. (1996) *J. Biol. Chem.* 271, 17593–17596
11. Olson, J. S., and Phillips, G. N., Jr. (1997) *J. Biol. Inorg. Chem.* 2, 544–552
12. Morikis, D., Champion, P. M., Springer, B. A., and Sligar, S. G. (1989) *Biochemistry* 28, 4791–4800
13. Tian, W. D., Sage, J. T., Champion, P. M., Chien, E., and Sligar, S. G. (1996) *Biochemistry* 35, 3487–3502
14. Peterson, E. S., Huang, S., Wang, J., Miller, L. M., Vidugiris, G., Kloek, A. P., Goldberg, D. E., Chance, M. R., Wittenberg, J. B., and Friedman, J. M. (1997) *Biochemistry* 36, 13110–13121
15. Cameron, A. D., Smerdon, S. J., Wilkinson, A. J., Habash, J., Helliwell, J. R., Li, T. S., and Olson, J. S. (1993) *Biochemistry* 32, 13061–13070
16. Quillin, M. L., Li, T. S., Olson, J. S., Phillips, G. N., Doy, Y., Ikeda-Saito, M., Regan, R., Carlson, M., Gibson, Q. H., Li, H. Y., and Elber, R. (1995) *J. Mol. Biol.* 245, 416–436
17. Antonini, E., and Brunori, M. (1971) *Hemoglobin and Myoglobin in Their Reactions With Ligands*, Elsevier/North-Holland Publishing Co., Amsterdam
18. Geraci, G., Parkhurst, L. J., and Gibson, Q. H. (1969) *J. Biol. Chem.* 244, 4664–4667
19. Boyer, P. D. (1954) *J. Am. Chem. Soc.* 76, 4331–4337
20. Duddell, D. A., Morris, R. J., and Richards, J. T. (1979) *J. Chem. Soc. Chem. Commun.* 75–76
21. Alpert, B., Mohsni, S. E., Lindqvist, L., and Tribel, F. (1979) *Chem. Phys. Lett.* 64, 11–16
22. Friedman, J. M., and Lyons, K. B. (1980) *Nature* 284, 570–572
23. Spiro, T. G. (1983) in *Iron Porphyrins* (Lever, A. B. P., and Gray, H. B., eds) Part II, pp. 89–159, Addison-Wesley Publishing Co., Reading, PA
24. Spiro, T. G., and Li, X.-Y. (1988) in *Biological Application of Raman Spectroscopy* (Spiro, T. G., ed) Vol. III, pp. 1–37, John Wiley & Sons, Inc., New York
25. Bangcharoenpaurpong, O., Schomacker, K. T., and Champion, P. M. (1984) *J. Am. Chem. Soc.* 106, 5688–5698
26. Kitagawa, T. (1988) in *Biological Application of Raman Spectroscopy* (Spiro, T. G., ed) Vol. III, pp. 97–131, John Wiley & Sons, Inc., New York
27. Rousseau, D. L., and Friendman, J. M. (1988) in *Biological Application of Raman Spectroscopy* (Spiro, T. G., ed) Vol. III, pp. 133–215, John Wiley & Sons, Inc., New York
28. Friedman, J. M. (1994) *Methods Enzymol.* 232, 205–231
29. Peterson, E. S., and Friedman, J. M. (1998) *Biochemistry* 37, 4346–4357
30. Friedman, J. M. (1985) *Science* 228, 1273–1280
31. Austin, R. H., Beeson, K. W., Eisenstein, L., Frauenfelder, H., and Gunsalus, I. C. (1975) *Biochemistry* 14, 5355–5373
32. Carlson, M. L., Regan, R., Elber, R., Li, H., Phillips, G. N., Jr., Olson, J. S., and Gibson, Q. H. (1994) *Biochemistry* 33, 10597–10606
33. Carlson, M. L., Regan, R. M., and Gibson, Q. H. (1996) *Biochemistry* 35, 1125–1136
34. Gibson, Q. H., Regan, R., Elber, R., Olson, J. S., and Carver, T. E. (1992) *J. Biol. Chem.* 267, 22022–22034
35. Scott, E. E., and Gibson, Q. H. (1997) *Biochemistry* 36, 11909–11917
36. Chernoff, D. A., Hochstrasser, R. M., and Steele, A. W. (1980) *Proc. Natl. Acad. Sci. U. S. A.* 77, 5606–5610
37. Jongeward, K. A., Magde, D., Taube, D. J., Marsters, J. C., Traylor, T. G., and

Sharma, V. S. (1988) *J. Am. Chem. Soc.* 110, 380–387
38. Friedman, J. M., Scott, T. W., Fisanick, G. J., Simon, S. R., Findsen, E. W., Ondrias, M. R., and MacDonald, V. W. (1985) *Science* 229, 187–190
39. Petrich, J. W., Poyart, C., and Martin, J. L. (1988) *Biochemistry* 27, 4049–4060
40. Morris, R. J., and Gibson, Q. H. (1980) *J. Biol. Chem.* 255, 8050–8054
41. Chance, M. R., Courtney, S. H., Chavez, M. D., Ondrias, M. R., and Friedman, J. M. (1990) *Biochemistry* 29, 5537–5545
42. Ahmed, A. M., Campbell, B. F., Caruso, D., Chance, M. R., Chavez, M. D., Courtney, S. H., Friedman, J. M., Iben, I. E. T., Ondrias, M. R., and Yang, M. (1991) *Chem. Phys.* 158, 329–351
43. Szabo, A., and Karplus, M. (1972) *Biochem. Biophys. Res. Commun.* 46, 855–860
44. Lim, M., Jackson, T. A., and Anfinrud, P. A. (1995) *Science* 269, 962–966
45. Lim, M., Jackson, T. A., and Anfinrud, P. A. (1995) *J. Chem. Phys.* 102, 4355–4366
46. Hofrichter, J., Henry, E. R., Sommer, J. H., Deutsch, R., Ikeda-Saito, M., Yonetani, T., and Eaton, W. A. (1985) *Biochemistry* 24, 2667–2679
47. Friedman, J. M., Scott, T. W., Stepnoski, R. A., Ikeda-Saito, M., and Yonetani, T. (1983) *J. Biol. Chem.* 258, 10564–10572
48. Scott, T. W., Friedman, J. M., and Macdonald, V. W. (1985) *J. Am. Chem. Soc.* 107, 3702–3705
49. Scott, T. W., and Friedman, J. M. (1984) *J. Am. Chem. Soc.* 106, 5677–5687
50. Smerdon, S. J., Dodson, G. G., Wilkinson, A. J., Gibson, Q. H., Blackmore, R. S., Carver, T. E., and Olson, J. S. (1991) *Biochemistry* 30, 6252–6260
51. Ackers, G. K., and Smith, F. R. (1985) *Annu. Rev. Biochem.* 54, 597–629
52. Kwiatkowski, L. D., Hui, H. L., Wierzba, A., Noble, R. W., Walder, R. Y., Peterson, E. S., Gibar, S. G., and Sanders, K. E. (1998) *Biochemistry* 37, 4325–4335
53. Friedman, J. M., Rousseau, D. L., and Ondrias, M. R. (1982) *Annu. Rev. Phys. Chem.* 33, 471–491
54. Li, T., Quillin, M. L., Phillips, G. N., Jr., and Olson, J. S. (1994) *Biochemistry* 33, 1433–1446
55. Li, X.-Y., and Spiro, T. G. (1988) *J. Am. Chem. Soc.* 110, 6024–6033
56. Spiro, T. G., and Kozlowski, P. M. (1997) *J. Biol. Inorg. Chem.* 2, 516–520